Reviewed Preprint
v1 • May 6, 2026
Not revised

Reviewed Preprint
v2 • October 27, 2026
Revised by authors

Selective suppression and biasing of chemokine receptors CCR9 and ACKR4 through targeting CCL25 with de novo miniproteins

Bas de Boer*, Thomas D Lamme*, Karlijn Verdwaald*, Sara Santamaria Medina, Csongor G Németh, Elisabeth M Elfrink, Martine J Smit, Iwan JP de Esch, Christopher T Schafer

Faculty of Science, Department of Chemistry and Pharmaceutical Sciences, Division of Medicinal Chemistry, Amsterdam Institute for Molecular and Life Sciences (AIMMS), Vrije Universiteit Amsterdam, Amsterdam, Netherlands

For correspondence: c.t.schafer@vu.nl

* contributed equally to the work

Competing interests: No competing interests declared

Funding: See page 21

Reviewing editor: Nevin A Lambert, Augusta University, United States

© 2026, de Boer et al. This article is distributed under the terms of the Creative Commons Attribution License, which permits unrestricted use and redistribution provided that the original author and source are credited.

eLife Assessment

This **important** study describes computationally designed proteins that bind to the chemokine CCL25. The authors present evidence that some binders simply prevent chemokine binding to the CCR9 receptor, while one binder changes the downstream signaling triggered by chemokine binding. The evidence is **convincing**, showing a degree of selectivity between chemokine ligands that could be further improved. The study will be of interest to pharmacologists, cell biologists studying chemokine function, and protein engineers.

https://doi.org/10.7554/eLife.111190.2.sa4

Abstract

Chemokines and their receptors mediate cell migration and coordinate immune responses, while dysregulation can lead to inflammation. Therapeutic modulation of the chemokine signaling axis has proven difficult. Most drug discovery efforts target the receptors, whereas natural regulatory mechanisms modulate immune responses by directly binding to or modifying the chemokine ligands. Despite this insight, development of effective chemokine-directed modulators has remained elusive. Recent advances in de novo protein design offer an unprecedented opportunity to produce high-affinity binders that efficiently block protein-protein interactions. We implemented a computational workflow leveraging the BindCraft platform to generate miniprotein binders against CCL25, the chemokine ligand for the receptors CCR9 and ACKR4 and implicated in inflammatory bowel diseases. The unbiased development results in several miniproteins designed to block the receptor N-terminus from wrapping the chemokine and prevent productive engagement. Thus, these proteins suppress CCL25-mediated effector coupling and halt MOLT-4 lymphoblast migration. Another class of miniprotein, represented by VUP25111, is predicted to bind CCL25 along the chemokine β1 strand and retained receptor binding. This complex inhibited arrestin recruitment to CCR9, but not to ACKR4, indicating receptor specificity. Additionally, G protein recruitment to CCR9 was unimpeded by VUP25111, suggesting that the miniprotein biased the native agonist towards G proteins. These results demonstrate the effectiveness of differentially targeting CCL25 to suppress CCR9 signaling and new tools to resolve the structural basis of chemokine receptor activation and bias.

Introduction

Chemokines are small secreted proteins (~10 kDa) that direct cell migration throughout the body by activating chemokine receptors, a subfamily of G protein-coupled receptors (GPCRs). The chemokine system plays critical roles in coordinating immune responses and homeostasis, as well

as directing cell positioning during development and wound repair [1]. Dysregulation of either the receptors or chemokines results in inflammatory diseases, cancer metastasis, and immune evasion of cancers and pathogens [2]. While attractive therapeutic GPCR targets, it has proven difficult to develop effective drugs towards chemokine receptors and only a few candidates have reached the clinic. This suggests that new targeting strategies are needed to fully exploit this versatile and promising signaling pathway [3,4].

The receptor:chemokine system comprises ~50 chemokines and ~20 receptors, forming an intricate web of cross-reactivity that allows for highly specific cell positioning [5]. Chemokine binding to chemokine receptors is often simplified to a two-site, two-step model, predominantly involving contacts with the receptor N-terminus and the orthosteric ligand-binding site in the transmembrane (TM) domain, termed chemokine recognition site (CRS) 1 and 2, respectively (Fig. 1A) [6–8]. Early models proposed that CRS1 would catch the chemokines and orient binding into CRS2 for receptor activation. Subsequent studies suggested that the ligands interact first with the TM domain of CRS2, and the N-terminus follows by wrapping around the chemokine to stabilize a higher affinity state [9]. Both sites are generally required for activation, with N-terminal receptor truncations or CRS2 point mutations being equally effective at impairing signaling responses [9–12]. Proper binding leads to GPCR activation and coupling of G protein and/or arrestin effector proteins.

The CC chemokine receptor 9 (CCR9) is expressed on thymocytes and intestinal lymphocytes [13,14] and promotes the migration of immune cells between the thymus and small intestine in response to its sole native agonist, CC chemokine CCL25 [15,16]. This receptor:chemokine pair regulates T cell development in the thymus and coordinates immune homeostasis and surveillance in the colon. Thus, overexpression and imbalance of this signaling axis are implicated in inflammatory bowel (IBD) and Crohn's diseases [17,18], as well as contributing to cancer metastasis to the gut [19,20]. Clinical development of CCR9 antagonists has thus far been unsuccessful, with efficacy in patients remaining a significant challenge [21].

Biological interference of the receptor:chemokine axis preferentially occurs at the level of the chemokine rather than the receptors. For example, pathogens and pests modulate immune responses targeting chemokines. To avoid the host's immune response, ticks have evolved small, salivary chemokine-binding proteins called evasins that block the chemokine interactions with receptors or glycosaminoglycans [22,23]. This action prevents the immune system from responding and impeding the tick's blood meal. Another, perhaps more cumbersome, way to target chemokines is by atypical chemokine receptors (ACKRs) that scavenge chemokines by internalizing the receptor:chemokine complex into the cell, thereby altering the chemokine gradients that are essential for chemokine-driven cell migration [24]. For example, CCL25 is an agonist for CCR9 but is scavenged by the atypical chemokine receptor ACKR4 [25]. These examples suggest that targeting the chemokine ligand may represent an effective mechanism for remodeling immune responses.

To study the chemokine receptor:chemokine axis in more detail, a variety of chemokine modulators is needed. However, these small proteins have proven challenging to target effectively using conventional approaches. For example, an NMR-based CCL28 fragment screen gave a low hit rate (<1%) of very weak affinity binders (Kd>1 mM) [26], thereby indicating low ligandability. We were therefore prompted to consider alternative approaches. With an avalanche of protein structural information becoming available, the use of de novo structure generation algorithms is making a revival. Recent advances in artificial intelligence-driven structure prediction have yielded highly accurate tools such as AlphaFold2 (AF2) [27]. Building on these developments, researchers have introduced de novo binder design frameworks that generate protein structures and sequences from scratch [28], including Chai-2 [29], AlphaProteo [30], and BindCraft [31]. The latter has emerged as a fully integrated, one-shot platform for binder design based only on an input target protein. BindCraft is an AF2-driven inverse-design pipeline that hallucinates binder sequences by backpropagating gradients through AlphaFold2-Multimer [32] and repredicting the binder-target complex at every iteration, enabling flexible co-optimization of sequence, structure, and interface. Designed binders are further refined using MPNNsol [33] and filtered based on AF2

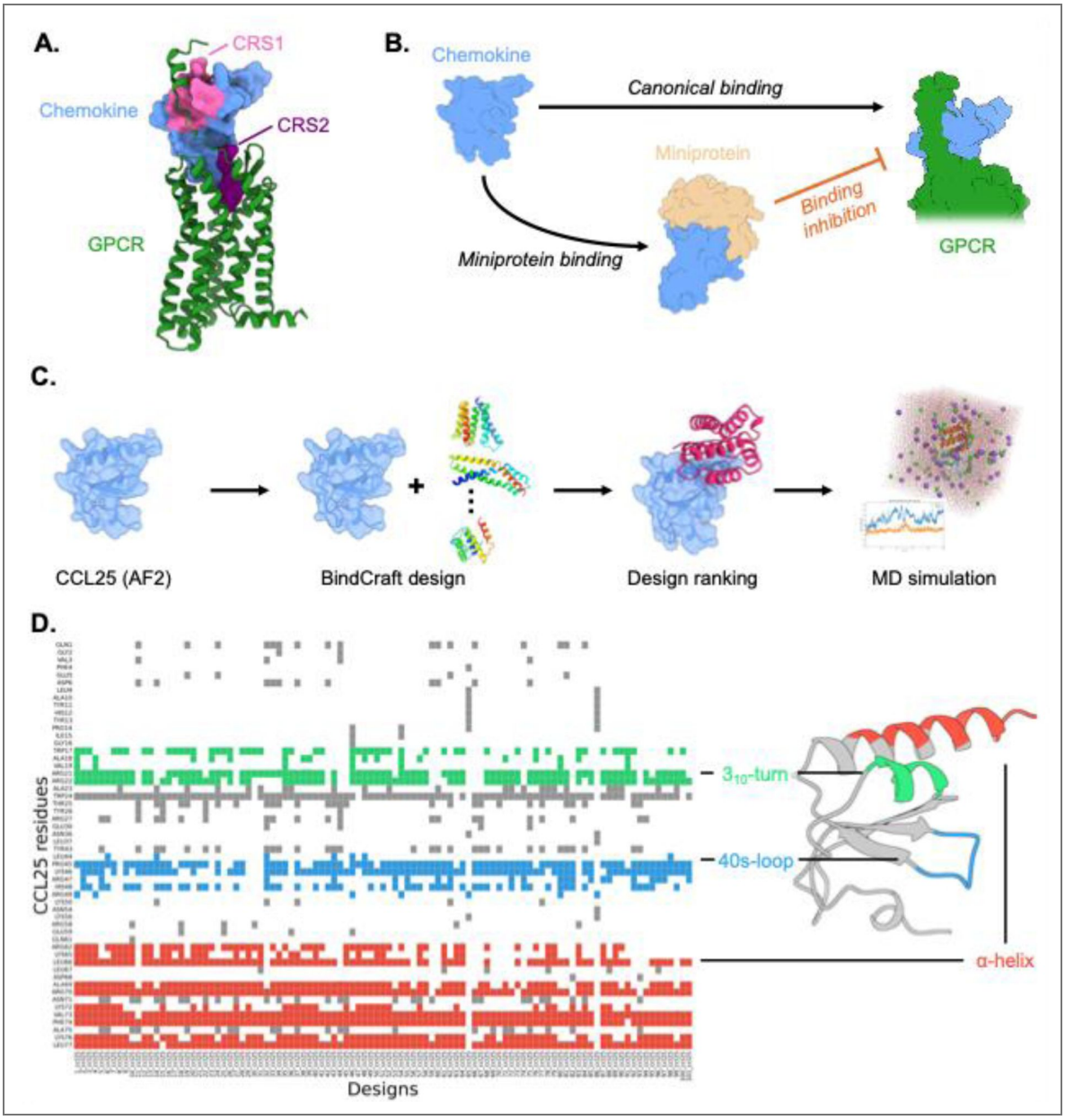


Figure 1. Design strategy and computational workflow for miniprotein binder design against CCL25.

(**A**) Chemokine interacts with chemokine receptors primarily through CRS1 (Pink, receptor N-terminus with chemokine body) and CRS2 (Purple, chemokine N-terminus with receptor TM domain). The receptor:chemokine complex is generated using AF3 with sequences of CCR9 and CCL25. (**B**) Conceptual framework illustrating the strategy for inhibiting canonical chemokine to receptor binding by directly targeting chemokine with designer miniprotein binders. (**C**) Computational workflow used to generate chemokine-binding miniproteins. (**D**) Molecular interaction map summarizing contacts between all miniprotein designs and CCL25. The most frequently targeted structural elements, the α-helix, the 3_{10}-turn, and the 40s-loop, are highlighted in red, green, and blue, respectively.

confidence and Rosetta [34] physics-based metrics. The platform's integrated workflow makes BindCraft easy to apply, lowering the barrier of entry for de novo binder design and enabling broad accessibility with a high success rate against a diverse set of targets [31,35,36].

Here, we apply BindCraft's de novo protein design to generate modulators for CCL25. Out of the generated BindCraft designs, four miniproteins were selected, produced, isolated and characterized. All show selective binding to CCL25 and form complexes that inhibit receptor activation. Most prevent activation by impeding chemokine binding to the receptor, thus impairing all signaling and migratory responses, but one forms a G protein-biased complex with CCL25, preserving G protein recruitment while suppressing arrestin recruitment to CCR9, and selectively inhibits CCR9, but not ACKR4. These results highlight the effectiveness of targeting chemokines with de novo protein modulators as unique research tools to probe the receptor:chemokine signaling axis.

Results

Generation of de novo miniprotein binders targeting CCL25

In order to generate binders against CCL25, the AF2-predicted model was obtained from the AlphaFold protein database [37]. CCL25 is the largest member of the chemokine family and contains a long C-terminal extension following the classic chemokine fold. To focus the miniprotein designs on the core chemokine domain to block CRS interactions and receptor binding (Fig. 1A, B), we performed our design efforts using a truncated form of the chemokine. The truncated CCL25 (CCL25_ΔCT, 1-77) activated both CCR9 and ACKR4 with similar efficacy while showing slightly enhanced potency only towards CCR9 compared to the full-length ligand (Fig. S1).

The overall workflow is presented in Fig. 1C. Starting from the CCL25 AlphaFold2 model, the BindCraft algorithm generates candidate designs of 75-125 amino acids with diverse structures. No predefined binding hotspots were imposed, and thus, designs were permitted to explore the entire CCL25 surface, allowing BindCraft to identify favorable interaction sites. At most two proteins with identical backbones were used for further processing to promote diversity among the designed binders. Following the design run, after 101 candidates passed computational filters, binders were ranked by the ipTM score.

Predicted complexes demonstrated robust prediction metrics, with ipTM scores (interface predicted TM-score) ranging from 0.55 to 0.87, ipAE scores (interface predicted aligned error) from 0.16 to 0.34, and pLDDT scores (predicted local distance difference test) from 0.83 to 0.95 (Fig. S2). Structural inspection revealed substantial backbone diversity among designs, although all adopted predominantly α-helical secondary structures (Fig. S3). Pairwise TM-score analysis yielded an average of 0.41, and UMAP projection of TM-score similarities confirmed broad structural dispersion (Fig. S3). Despite the absence of a predefined binding hotspot, most designs target a region encompassing one face of the α-helix, the 3_{10}-turn, and the 40s-loop with large structural diversity (Fig. 1D). As a last step, we subjected the top 20 miniprotein designs to 100 ns MD simulations to assess complex stability. Calculation of the backbone RMSD of the binders reveals good stability for all complexes, and estimation of binding free energy using the MM/GBSA method [38] furthermore predicts favorable binding complexes of all top 20 miniproteins (Table S1).

De novo designed binders target CCL25 with high affinity

From the top 20 scored binders, four were selected for insertion into expression vectors for *E. coli* purification based on predicted binding energies, diversity of structural scaffolds, and binding interfaces (Fig. 2A, Table S1). Three of the four VU miniproteins (VUPs), VUP25101, VUP25107, and VUP25112, are predicted to interact with the C-terminal helix of the chemokine, blocking CRS1 interactions and opposite the GPCR transmembrane bundle. The fourth, VUP25111, makes unique interactions compared to the others (Fig. S4) and is predicted to bind along the β1 strand and 40s-loop of CCL25 without substantially impairing either CRS1 or CRS2 binding interfaces. The

binding of the designed miniproteins to CCL25 was validated by fluorescence polarization spectroscopy (FP) of a fluorophore (AZ488) attached to the C-terminus of full-length CCL25. An increase in the polarization of the fluorophore emission is the result of a decrease in the tumbling rate during fluorophore excitation and is reflective of an increase in the size of the protein complex due to miniprotein binding (Fig. 2B). All four tested binders produced an increase in polarization, indicating that the miniproteins indeed bind the CCL25 target (Fig. 2C). Similar affinity values were calculated for all four VUPs (VUP25101: pK_d = 6.42 ± 0.74, VUP25107: pK_d = 6.82 ± 0.43, VUP25111: pK_d 6.36 ± 0.35, VUP25112: pK_d = 6.30 ± 0.41). Importantly, these results also confirm that the miniproteins bind the full-length CCL25 chemokine despite being designed against an artificially truncated form, CCL25_ΔCT.

Miniproteins block CCL25 binding to CCR9 and ACKR4

As the miniproteins designed against CCL25 bind the desired chemokine in purified form, we next determined whether the CCL25-miniprotein complex inhibits binding to the receptor as intended. Binding of CCL25 to CCR9 or ACKR4 was determined by Time-Resolved Fluorescence Resonance Energy Transfer (TR-FRET) between a lanthanide donor attached to a SNAP-tag fused to the receptor N-terminus and a fluorophore on the C-terminus of CCL25 (AZ647) (Fig. 3A). CCL25_ΔCT was used in place of the full-length chemokine to shorten the distance between the donor and acceptor and improve energy transfer efficiency. Incubating CCL25 with three of the miniproteins, VUP25101, VUP25107, and VUP25112, impaired binding to CCR9 resulted in a complete loss of FRET at high miniprotein concentration (Fig. 3B). For ACKR4, VUP25101 and VUP25107 exhibit comparable inhibitory potencies, whereas VUP25112 is slightly reduced (Fig. 3C). Together, these these findings confirm that the miniproteins act as potent inhibitors by directly interfering with CCL25 binding to the receptors. VUP25111 shows a drastically lower inhibitory potency compared to the other binders and did not completely eliminate the binding signal. Since the binder readily complexes with the chemokine at these concentrations (Fig. 2), this suggests that the CCL25:VUP25111 complex retains some ability to interact with the receptor.

To explore a possible structural explanation for how the binders prevent CCL25 from engaging its receptors, we modeled the CCR9:CCL25 and ACKR4:CCL25 complexes using AlphaFold3 [39]. Superimposing the miniprotein:CCL25 complexes onto the predicted receptor:chemokine complexes reveals steric clashes in CRS1 between VUP25101, VUP25107, and VUP25112 and the N-terminus of both CCR9 and ACKR4 (Fig. 3D). This suggests that disrupting solely these contacts is sufficient to block proper receptor:chemokine complex formation. In contrast, superimposing the VUP25111:CCL25 complex on the models shows only minor clashes with the extracellular loop 2 (ECL2) of CCR9 and no predicted conflicts with ACKR4. Together, these results indicate that blocking CRS1 interactions between the receptor N-terminus and chemokine body robustly prevents CCL25 binding to both its canonical and atypical receptors, while targeting the β1-strand appears structurally tolerated.

De novo miniproteins inhibit CCL25-mediated arrestin recruitment to CCR9 and ACKR4

The effect of CCL25-targeting on receptor activation was first evaluated by assessing arrestin recruitment. Both CCR9 and ACKR4 show robust engagement with arrestins following agonist stimulation and serve as simple readouts of changes in receptor activation [40,41]. Thus, β-arrestin2 recruitment to the receptors was measured by BRET between a C-terminal luciferase fusion on the receptor (RlucII) and an N-terminal GFP10 on β-arrestin2 (Fig. 4A). In both cases, the addition of chemokine leads to a substantial increase in resonance energy transfer, indicating translocation of the effector in response to agonist-mediated receptor activation (Fig. 4B, C). Adding an increasing concentration of the miniprotein binders with a constant 20 nM CCL25 (Full-Length) progressively decreased the CCL25-promoted activation and all binders completely inhibited CCR9-arrestin recruitment at the highest concentrations (Fig. 4B). VUP25101, VUP25107, and VUP25112 showed similarly effective suppression of CCL25-mediated activation of CCR9 (VUP25101: pIC_{50} = 7.92 ± 0.07; VUP25107: pIC_{50} = 8.01 ± 0.24; VUP25112: pIC_{50} = 7.56 ± 0.41).

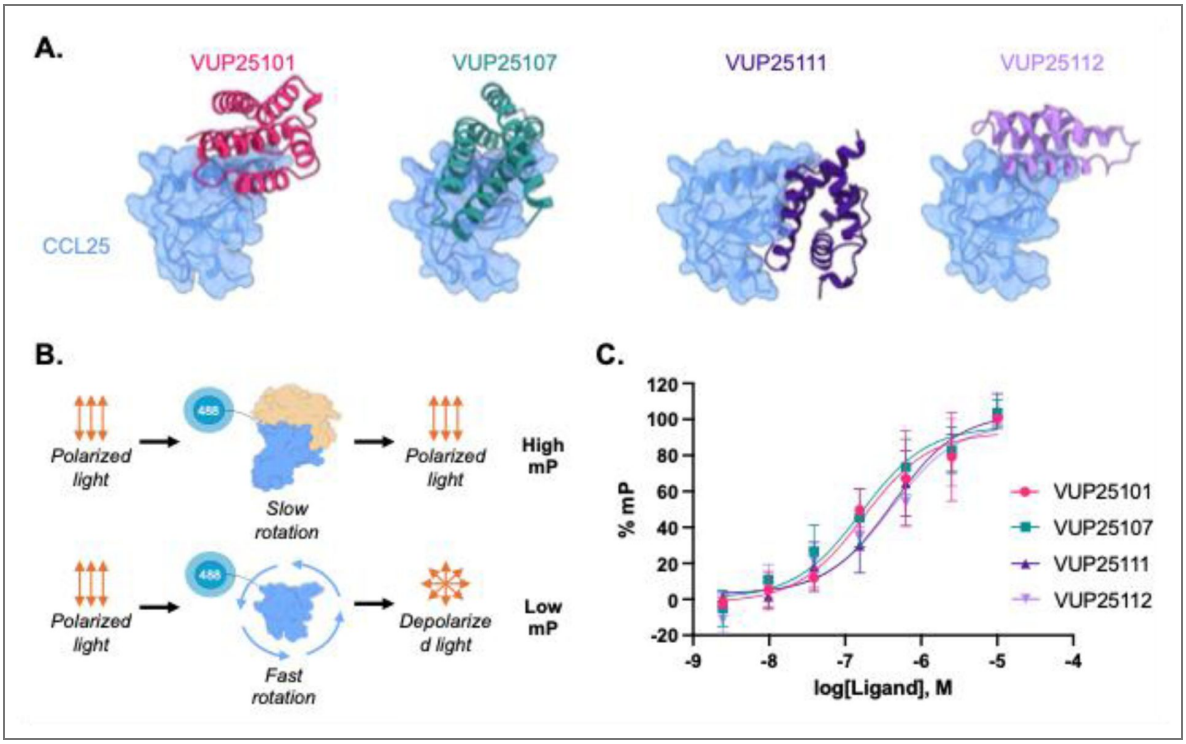


Figure 2. VUPs (VU miniproteins) are confirmed to directly bind CCL25.

(**A**) Structural models of the generated designs for CCL25. CCL25 is shown in blue with a surface representation, and the binders are displayed as cartoon in various colors. (**B**) Cartoon schematic for the fluorescence polarization assay. When the miniprotein binds CCL25_AZ488, the size increases, as does the polarization of the emitted light. (**C**) The polarized fluorescent emission was measured for 15 nM CCL25_AZ488 in the presence of increasing concentrations of VUP binders. Binding of the miniproteins leads to an increase in polarization. Data points represent the average ± SD of three independent experiments and internally normalized to the minimum and maximum polarization of each binder.

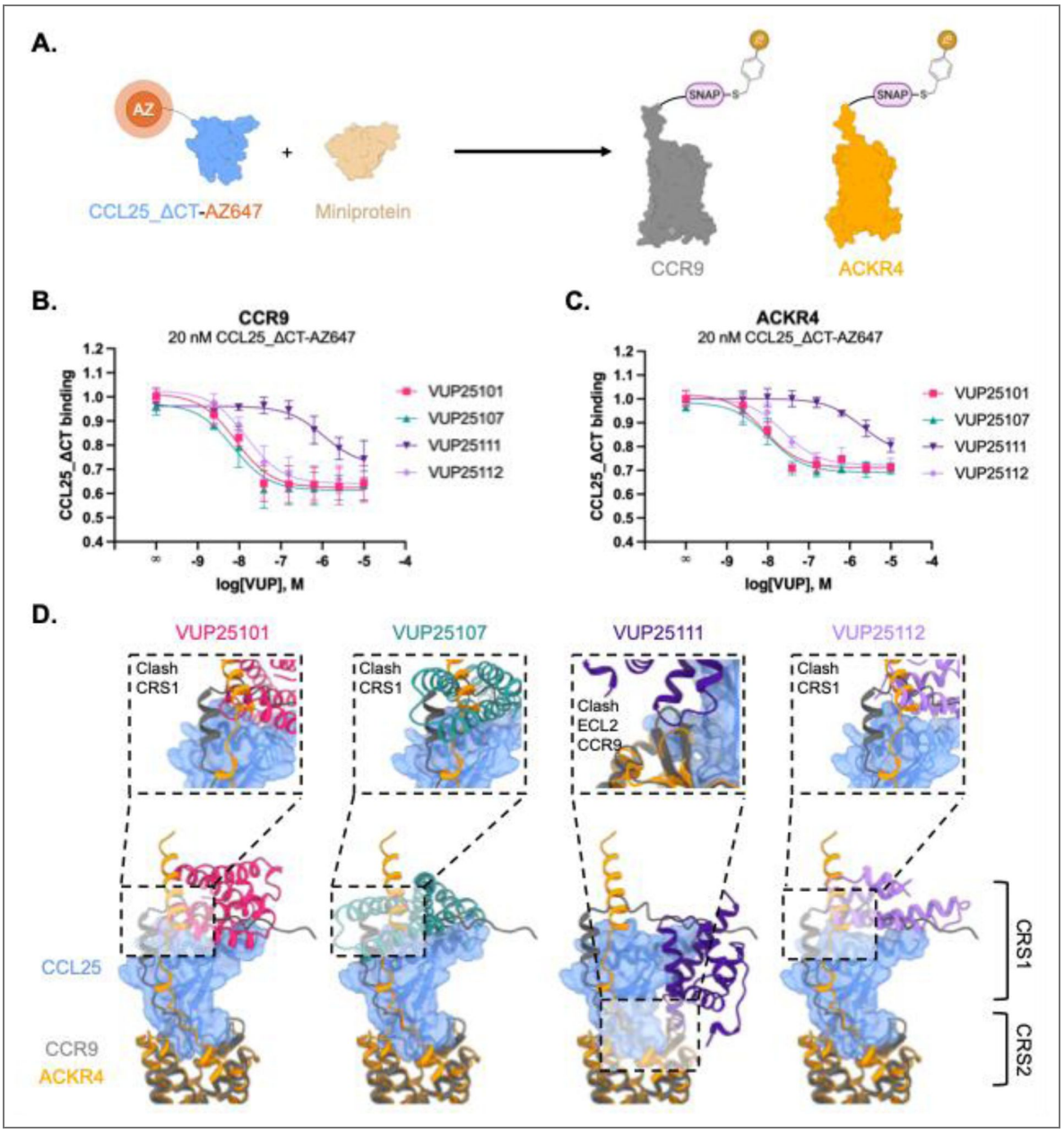


Figure 3. VUPs interfere with CCL25 binding to CCR9 and ACKR4 through clashes with CRS1.

(**A**) Design of binding assay using TR-FRET between CCL25_ΔCT-AZ647 and terbium (Tb) labelled SNAP-CCR9 and SNAP-ACKR4. TR-FRET binding results for CCR9 (**B**) and ACKR4 (**C**) using 20 nM CCL25_ΔCT-AZ647 with increasing concentrations of the miniproteins, which shows a decreasing TR-FRET signal indicating an inability of the chemokine:VUP complex from binding the target receptor. Values represent the mean ± SD of three independent experiments performed in triplicate, presented as fold over vehicle condition. Significance was determined using Extra sum-of-squares F test with VUP25101 as a reference, *P < 0.01, **P < 0.0001. (**D**) Predicted structural models of miniproteins superimposed on the AF3-predicted CCR9:CCL25 (dark blue cartoon) and ACKR4:CCL25 (golden cartoon) complexes with zoom-in panels highlighting where the miniproteins are predicted to sterically clash with receptor:chemokine models.

The IC_{50} of VUP25111 was dramatically shifted by 2 log units (pIC_{50} = 5.77 ± 0.33). Given the different binding mode of VUP25111 to CCL25 (Fig. 3D), this indicates that the mechanism by which VUP25111 inhibits CCR9 activation may also differ.

CCL25-mediated arrestin recruitment to ACKR4 was also robustly inhibited by VUP25101 (pIC_{50} = 7.73 ± 0.74) and VUP25107 (pIC_{50} = 7.71 ± 0.43) (Fig. 4C). VUP25112 also completely impaired CCL25-mediated activation of the atypical receptor at the highest concentrations, but with significantly less potency (pIC_{50} = 6.95 ± 0.34) compared to VUP25101 and VUP25107 (Table S2). The unique binder VUP25111, on the other hand, did not significantly impact the activation of ACKR4 by CCL25 at any tested miniprotein concentration. The lack of effect supports the structural interpretation that the CCL25:VUP25111 complex can bind ACKR4 as a cooperative unit and implies that this complex also does not alter the receptor's native, chemokine-promoted activation. These data indicate that CCL25-activation of both CCR9 and ACKR4 can be efficiently inhibited by targeting the CRS1-binding interface and suggest sufficient differences in the CCL25:receptor interface that allow receptor-specific inhibition.

CCL25 specificity was experimentally evaluated by testing the miniproteins against CXCL12 by tracking arrestin recruitment to CXCR4 and ACKR3, the native agonist for this canonical and atypical receptor pair (Fig. S5). VUP25111 and VUP25112 showed no effect on CXCL12-mediated activation at any concentration, while VUP25101 and VUP25107 showed partial inhibition at the highest tested concentration (10 μM).

In addition, the effects of the VUPs were evaluated against CCL20, a closely related chemokine to CCL25, by assessing arrestin recruitment to CCR6 and ACKR4 (Fig. S6). VUP25107 and VUP25112 displayed similar inhibitory potencies of CCL20 as to CCL25 for ACKR4 (VUP25107: pIC50 = 7.72 ± 0.21; VUP25112: pIC50 = 6.93 ± 1.03). In contrast, VUP25101 showed reduced inhibition of CCL20 relative to CCL25 (VUP25101: $pIC50_{CCL20}$ = 6.06 ± 0.13 v $pIC50_{CCL25}$ = 7.73 ± 0.08), indicating greater selectivity for the designed target. CCL20 activation of CCR6 further supports the specificity of VUP25101, which only showed a modest effect at the highest concentration tested. VUP25111 showed no inhibitory effects on CCL20 activation of either CCR6 nor ACKR4, which may indicate a lack of binding to the chemokine, but is also indiscernible from forming a receptor competent complex similar to the proposed CCL25:VUP25111:ACKR4 interaction.

G protein activation by CCR9 is inhibited by VUP25101, VUP25107, and VUP25112, but not VUP25111

Immune cell migration is driven in part by G protein coupling, thus, inhibition of this function is critical for crafting immune responses. The ability of the de novo binders to impact canonical G protein coupling was tested first by measuring the recruitment of 'mini' G proteins (mG_i), engineered Ras domain from $G\alpha_s$ with the interacting residues of G_i [42], to CCR9 by BRET between CCR9 C-terminally tagged with RlucII and mG_i fused to a Venus fluorophore (Fig. 5A). Like with arrestin recruitment, both VUP25101 and VUP25107 inhibited CCL25-induced mGi recruitment with similar potency (VUP25101: pIC_{50} = 8.17 ± 0.21; VUP25107: pIC_{50} = 8.44 ± 0.17) (Fig. 5B). Despite potent inhibition of arrestin engagement, VUP25112 showed a right-shifted IC_{50} value compared to the VUP25101 and VUP25107 (pIC_{50} = 7.15 ± 0.51). Interestingly, VUP25111 showed no effect on the mG_i recruitment even at concentrations that robustly inhibited arrestin engagement. The deviations between the arrestin results (Fig. 4) and G protein (Fig. 5B) suggest that the specific ligand interactions or receptor conformations driving arrestin engagement with CCR9 may be more strict than for the G proteins.

GPCR signaling is amplified by a cascade and altered recruitment of the G protein effector may not be reflected in downstream outputs. CCR9 is G_i-coupled and activation inhibits the production of cAMP and decreases the total concentration. The impact of the miniproteins on G protein signaling by CCR9 was monitored using a BRET-based cAMP biosensor (CAMYEL) to detect the inhibition of forskolin (FSK)-induced cAMP production (Fig. 5C). Downstream signaling was inhibited similar to mG_i recruitment, confirming the CCL25-targeting proteins are effective neutralizers of the chemokine-mediated signal (Fig. 5D). Despite the higher potency of CCL25 for cAMP inhibition

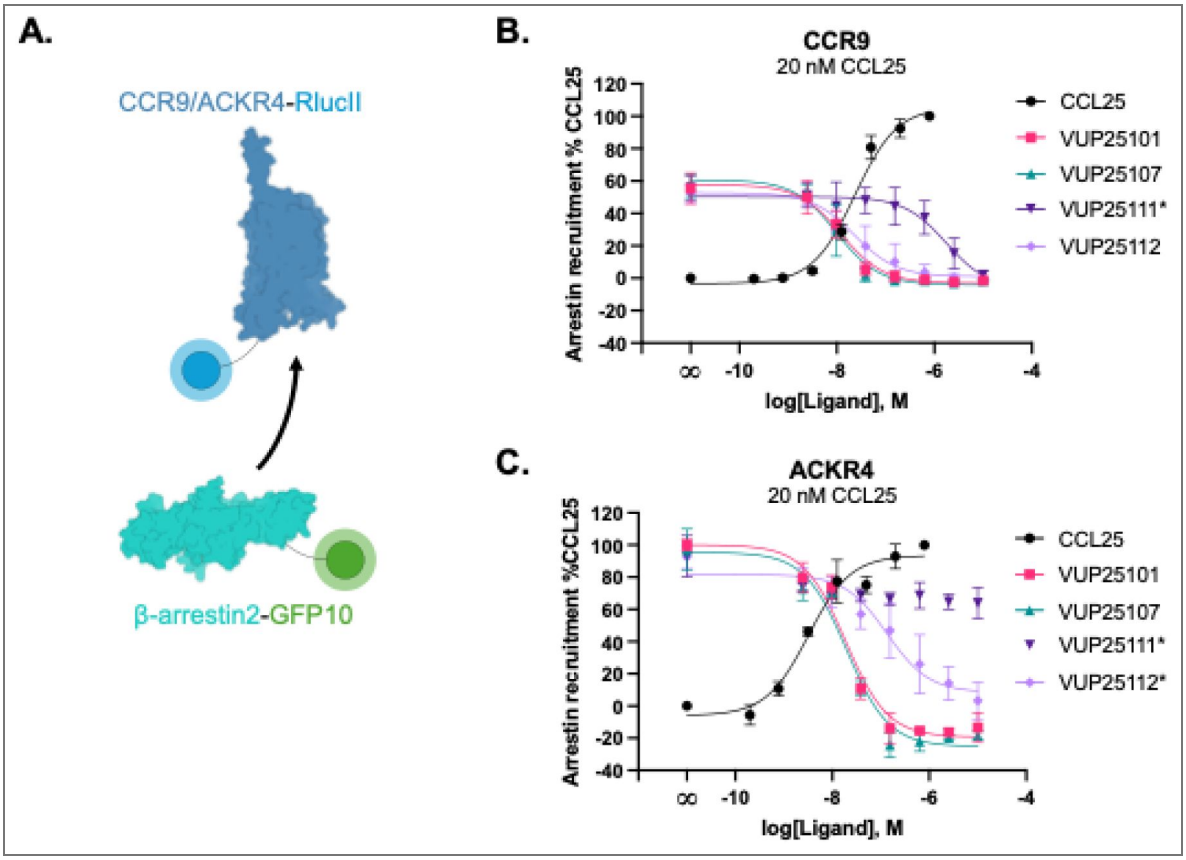


Figure 4. VUPs selectively inhibit CCL25-induced arrestin recruitment towards CCR9 and ACKR4.

(**A**) Schematic illustration of BRET sensor pair CCR9/ACKR4-RlucII and GFP10-β-arrestin2. The structure of β-arrestin2 is generated using AF3. β-Arrestin2 recruitment towards CCR9 (**B**) or ACKR4 (**C**) following stimulation across a titration of CCL25 concentrations (black) or a fixed concentration of CCL25 (20 nM) preincubated with increasing concentration of miniprotein. Values represent the mean ± SD of three independent experiments performed in duplicate and normalized to min and max CCL25 response. Significance was determined using Extra sum-of-squares F test with VUP25101 as a reference. *P < 0.0001.

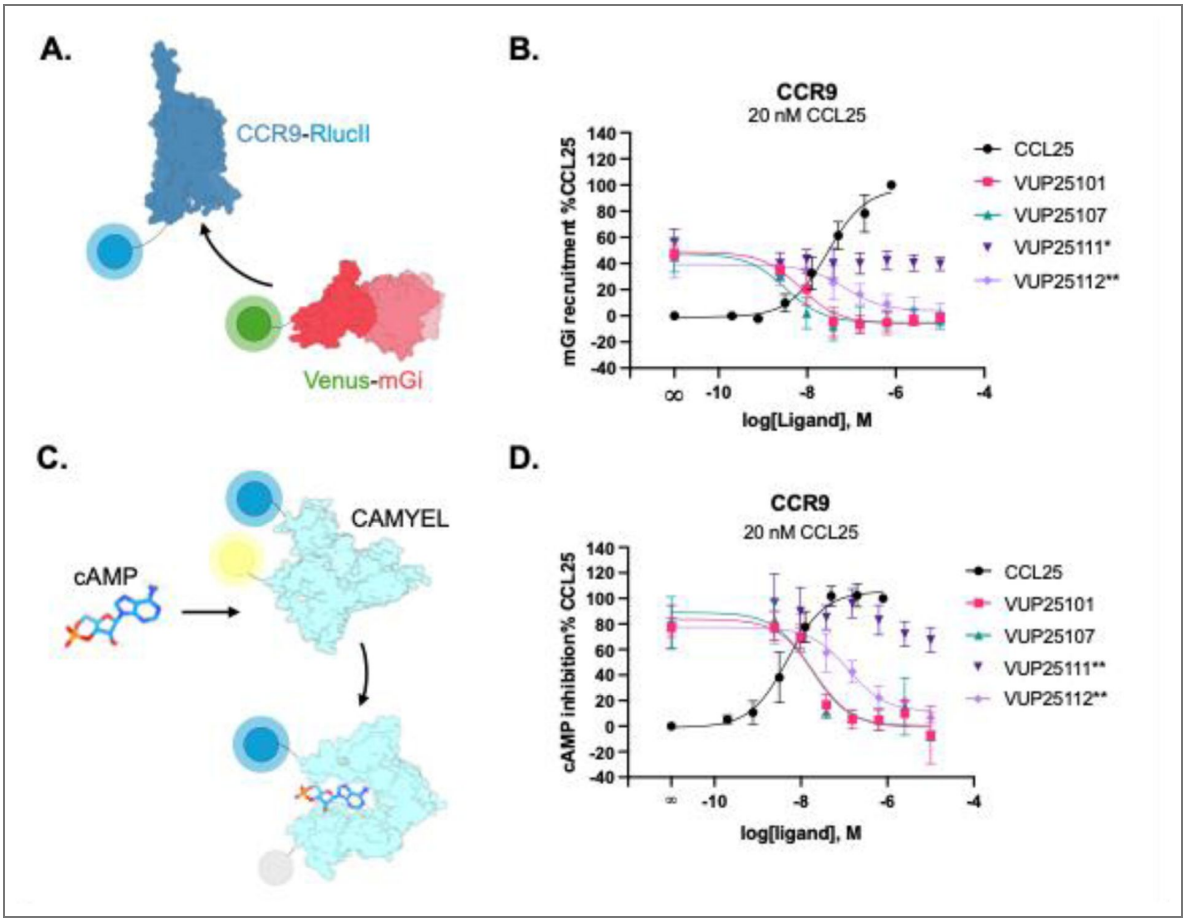


Figure 5. Most VUPs, but not VUP25111, effectively inhibit CCL25-induced G_i protein activation.

(**A**) Schematic illustration of BRET pair sensor CCR9 and Venus-mG_i. The complex representing mGi is taken from PDB 9KO4 [45]. (**B**) Concentration-dependent mG_i recruitment to CCR9 following stimulation with a titration of CCL25 (black) or with 20 nM CCL25 preincubated with increasing concentrations of miniproteins. (**C**) Suppression of cAMP signaling monitored by the BRET-based cAMP sensor CAMYEL. The structure of CAMYEL is generated using AF3. (**D**) CCR9 induced cAMP suppression following stimulation with a titration of CCL25 (black) or a fixed concentration of CCL25 (20 nM) preincubated with a titration of miniproteins. Values represent mean ± SD of three independent experiments performed in duplicate, normalized to min and max CCL25 response. Significance was determined using Extra sum-of-squares F test with VUP25101 as a reference, *P < 0.01 **P < 0.005.

compared to arrestin recruitment, a fixed concentration of 20 nM CCL25 was used throughout this and subsequent assays to maintain a consistent CCL25:miniprotein stoichiometry. As this concentration represents different points on the respective concentration-response curves, cross-assay comparisons of apparent miniprotein potency should be interpreted qualitatively. Like with mG_i, VUP25111 did not impact cAMP inhibition at any concentration, further confirming that the binder is not affecting G protein activation. Taken together with the complete suppression of arrestin recruitment, it appears that the binding of VUP25111 converts the balanced natural agonist CCL25 to G protein-biased towards CCR9.

VUP25111:CCL25 only partially impairs GPCR kinase 3 translocation to CCR9

The preserved G protein response from CCR9 (Fig. 5) when treated with the VUP25111:CCL25 complex suggests greater complexity to how the miniprotein suppresses arrestin interactions. Arrestins are recruited to activated CCR9, like other GPCRs, following phosphorylation of the receptor C-terminus by GPCR kinases (GRKs) [41]. Thus, translocation readouts as seen in Fig. 4 report the combination of arrestin engagement and GRK phosphorylation and alterations to either event impact the response. To resolve if VUP25111 impairs the CCL25-mediated arrestin response through GRK phosphorylation, we measured the impact of the miniprotein binders on GRK3 recruitment to CCR9 by BRET between a nanoluciferase (Nluc) on GRK3 and a fluorophore (mV) on the receptor C-terminus (Fig. 6A). We have previously shown that, while all GRKs contribute of CCR9 phosphorylation, GRK3 shows the largest change in BRET upon recruitment to CCR9 [41]. Similar to G protein and arrestin, the miniproteins which interfere with CRS1 interactions, VUP25101, VUP25107, and VUP25112, also prevent chemokine-induced relocation of GRK3 to CCR9 with similar inhibitory potency as arrestin and G proteins (VUP25101: pIC_{50} = 8.40 ± 0.04; VUP25107: pIC_{50} = 8.32 ± 0.10; VUP25112: pIC_{50} = 7.81 ± 0.46) (Fig. 6B). Unexpectedly, VUP25111 treatment only partially inhibited GRK3 recruitment, but not the complete inhibition observed for these concentrations with arrestin recruitment. This suggests that either activation of CCR9 by the VUP25111:CCL25 complex promotes a conformation incompatible with arrestin engagement, but still accessible for GRK phosphorylation, or the reduced GRK interaction represents the formation of a phosphorylation barcode incapable of supporting arrestin recruitment. Without direct phosphorylation measurements these possibilities cannot be separated.

Targeting CCL25 with miniproteins inhibit CCR9 internalization

GRK phosphorylation largely drives CCR9 internalization through coordinating arrestins as well as a not fully-described phosphorylation dependent mechanism [41]. CCR9 internalization was tracked by BRET between CCR9-RlucII and a fluorophore (rGFP) anchored at the plasma membrane via a CAAX domain (rGFP-CAAX) (Fig. 7A) [43]. Receptor trafficking away from the surface is then reported as a decrease in the BRET. Binding of VUP25101, VUP25107, or VUP25112 with CCL25 potently prevented the chemokine-mediated endocytosis of CCR9 (VUP25101: pIC_{50} = 8.30 ± 0.12; VUP25107: pIC_{50} = 8.35 ± 0.16; VUP25112: pIC_{50} = 8.04 ± 0.33) (Fig. 7B). Internalization was also blocked fully by VUP25111, albeit at substantially lower inhibitory potency (pIC_{50} = 5.09 ± 0.27). These results suggest that the VUP25111:CCL25 complex suppresses both the arrestin dependent and independent internalization mechanisms used by CCR9, despite likely allowing for some, albeit perhaps insufficient, GRK phosphorylation.

Immune cell migration is inhibited by targeting CCL25 at the CRS1 interface

The goal of targeting CCL25 is to shape the CCR9-driven immune response to address inflammatory diseases of the bowels and inhibit CCR9-mediated metastasis of cancer cells. Migration of MOLT-4 cells, T lymphoblasts with native CCR9 expression (lacking significant ACKR4 expression [44]), was detected in a transwell format and quantified by counting the cells in the lower chamber with flow cytometry. The CCL25 concentration corresponding to the peak migratory signal (Fig. 8A) was added to the lower chamber with binder and total migrated cells

Figure 6. CCL25-mediated GRK3 recruitment to CCR9 is suppressed by VUP25101, VUP25107, and VUP25112, but not VUP25111.

(**A**) Schematic presentation of the GRK3 recruitment BRET setup to detect GRK3-Nluc translocation to activated CCR9-mV. (**B**) Recruitment of GRK3 to CCR9 measured by BRET across a concentration range of either CCL25 (black) or VUP miniproteins with a constant 20 nM CCL25. Values represent mean ± SD of three independent experiments performed in duplicate, normalized to min and max CCL25 response. Significance was determined using Extra sum-of-squares F test with VUP25101 as a reference, *P < 0.0001.

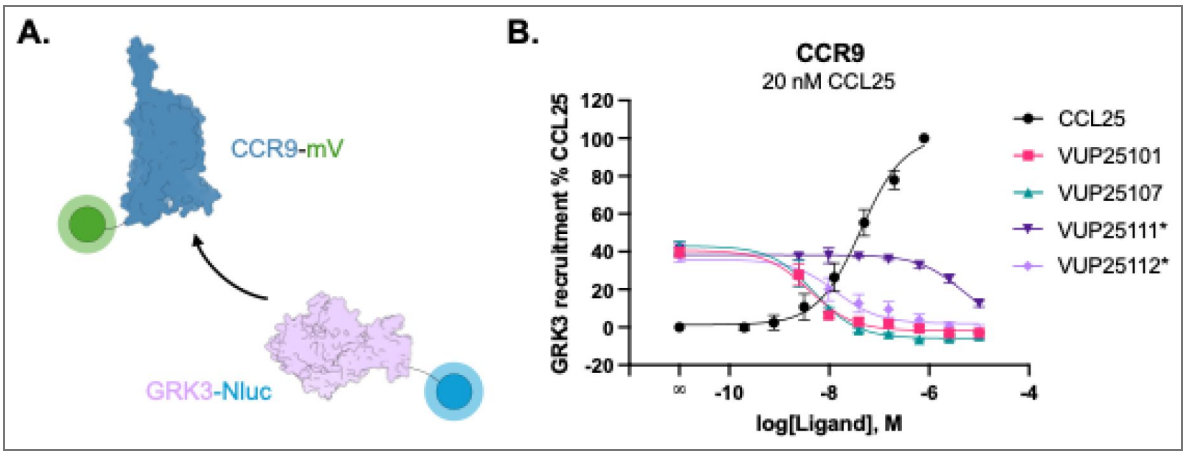
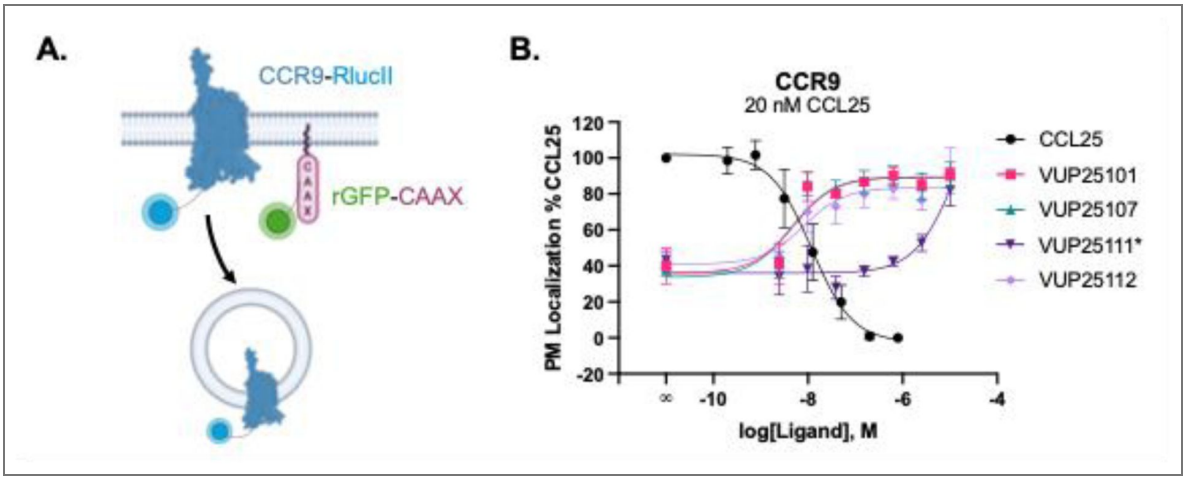


Figure 7. All VUPs inhibit CCL25-promoted internalization of CCR9.

(**A**) Schematic representation of the BRET assay to track CCR9 internalization by monitoring the resonance energy transfer between CCR9-RlucII and rGFP-CAAX. The BRET between the probes decreases as the receptor trafficks away from the membrane through internalization. (**B**) Internalization response measured by the BRET setup presented in (**A**) across a range of concentrations of CCL25 (black) or VUP miniproteins with 20 nM CCL25. Values represent the mean ± SD of three independent experiments performed in duplicate, normalized to min and max CCL25 response. Significance was determined using Extra sum-of-squares F test with VUP25101 as a reference. *P < 0.0001.



were counted after 2 hours. Like with the G protein assays in Fig. 5, VUP25101 and VUP25107 severely impaired the CCL25-mediated migration of CCR9-expressing immune cells (Fig. 8B). VUP25112 was less effective at inhibiting migration, as half of the migratory response towards CCL25 was still present, reflecting a similar relative level of inhibition as observed for G protein coupling. MOLT-4 cell migration was unaffected by the inclusion of VUP25111, consistent with the apparent G protein bias imparted by this binder to CCL25. These results demonstrate conclusively the effectiveness of miniproteins targeting the CRS1 interaction between CCR9 and CCL25. Such targeting impairs immune cell motility and has the potential to modify immune responses.

Discussion

Dysregulation of the CCL25:CCR9 signaling axis has been implicated in promoting inflammatory diseases of the gut [17,18] and contributing to cancer metastasis [19,20]. Although several CCR9 antagonists have been developed [46,47], none have passed clinical trials [21]. Recent advances in protein structure prediction enable accurate modeling of protein complexes and the de novo design of proteins with specific functions [48,49]. Because chemokines have proven difficult to target with small molecules, they represent an excellent application for these new protein design approaches.

Using BindCraft, miniproteins were designed to target CCL25. The miniproteins VUP25101, VUP25107, and VUP25112 were predicted to interact with the CCL25 surface involved in CRS1 interactions and robustly inhibited CCR9 and ACKR4 activation. This suggests that blocking contacts between CCL25 and the receptor N-terminus is sufficient to suppress chemokine-mediated signaling without directly targeting the receptor or its orthosteric binding pocket. Other chemokine interfaces, such as those involved in GAG binding or chemokine oligomerization, may similarly provide opportunities for modulating receptor activation. Unexpectedly, targeting CCL25 along the chemokine β1 strand, in the case of VUP25111, resulted in a miniprotein that inhibited CCR9-induced arrestin recruitment, but not G protein activation, and showed no inhibition of ACKR4. Thus, targeting CCL25 produced not only potent inhibitors, but also presented new insights into signaling along the receptor:chemokine axis (Fig. 9). Structural modeling suggests that when complexed with CCL25, VUP25111 would clash with the ECL2 of CCR9, whereas the three-residue-shorter loop of ACKR4 can accommodate the complex. Binding and G protein activation results suggest that VUP25111 does not prevent CCL25 from binding CCR9, but instead modifies the agonist interactions to become G protein-biased, as discussed further below. Selectively inhibiting the canonical receptor without impairing its atypical partner would suppress migratory signaling without disrupting chemokine scavenging. Blocking this regulatory mechanism may increase chemokine levels, dysregulate the signaling axis, and eventually overwhelm the inhibitors. Thus, continual removal of the agonist through native scavenging may be a necessary consideration when designing chemokine-targeting therapeutic.

Biased signaling with regard to GPCRs generally refers to preferential coupling to either G proteins or arrestins and can arise from specific ligands, receptor activation mechanisms, or cellular environment. VUP25111 prevents CCL25-induced arrestin recruitment to CCR9 but leaves G protein signaling intact. To our knowledge, this represents the first designed binder to alter the signaling bias of a natural ligand. The fact that the same ratio of binder to chemokine impairs arrestin coupling, but not G protein (Fig S8), indicates that the VUP25111:CCL25 complex is able to bind and activate CCR9. While GRK recruitment is partially suppressed, the lack of complete inhibition likely indicates that the kinases can phosphorylate the VUP25111:CCL25-activated receptor. The extent of phosphorylation is not clear and the inhibited GRK recruitment may reflect the formation of sub-phosphorylated states which cannot support arrestin recruitment, nor promote efficient receptor internalization. Alternatively, the miniprotein:chemokine complex may induce a conformational state incompatible with arrestin engagement. Due to the clash with ECL2, the loop would need to distort to accommodate the larger ligand complex and this displacement may translate into the G protein and GRK permissive structural state. A similar signaling profile with intact G protein but no arrestin coupling was recently observed by a CCR9 point mutation ($T208^{5.32}A$) immediately following ECL2 [50], however, we were unable to replicate these dramatic

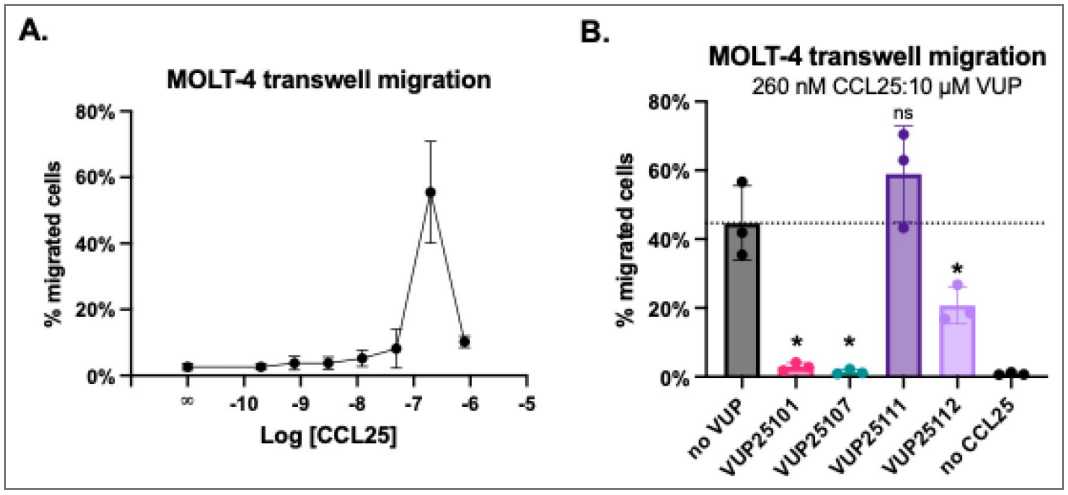


Figure 8. MOLT-4 chemotactic response towards CCL25 is suppressed by VUP binding.

(**A**) Percentage of migrated cells towards CCL25 across a titration of chemokine concentrations. (**B**) Percentage of migrated cells towards a fixed concentration of CCL25 (260 nM, corresponding to the highest migration observed in (**A**)) preincubated with miniproteins (10 µM). Values represent the mean ± SD of three independent experiments measured in technical triplicates by flow cytometry. Significance was determined using Welch ANOVA followed by a Dunnett's multiple comparisons test comparing to no VUP. *p<0.05.

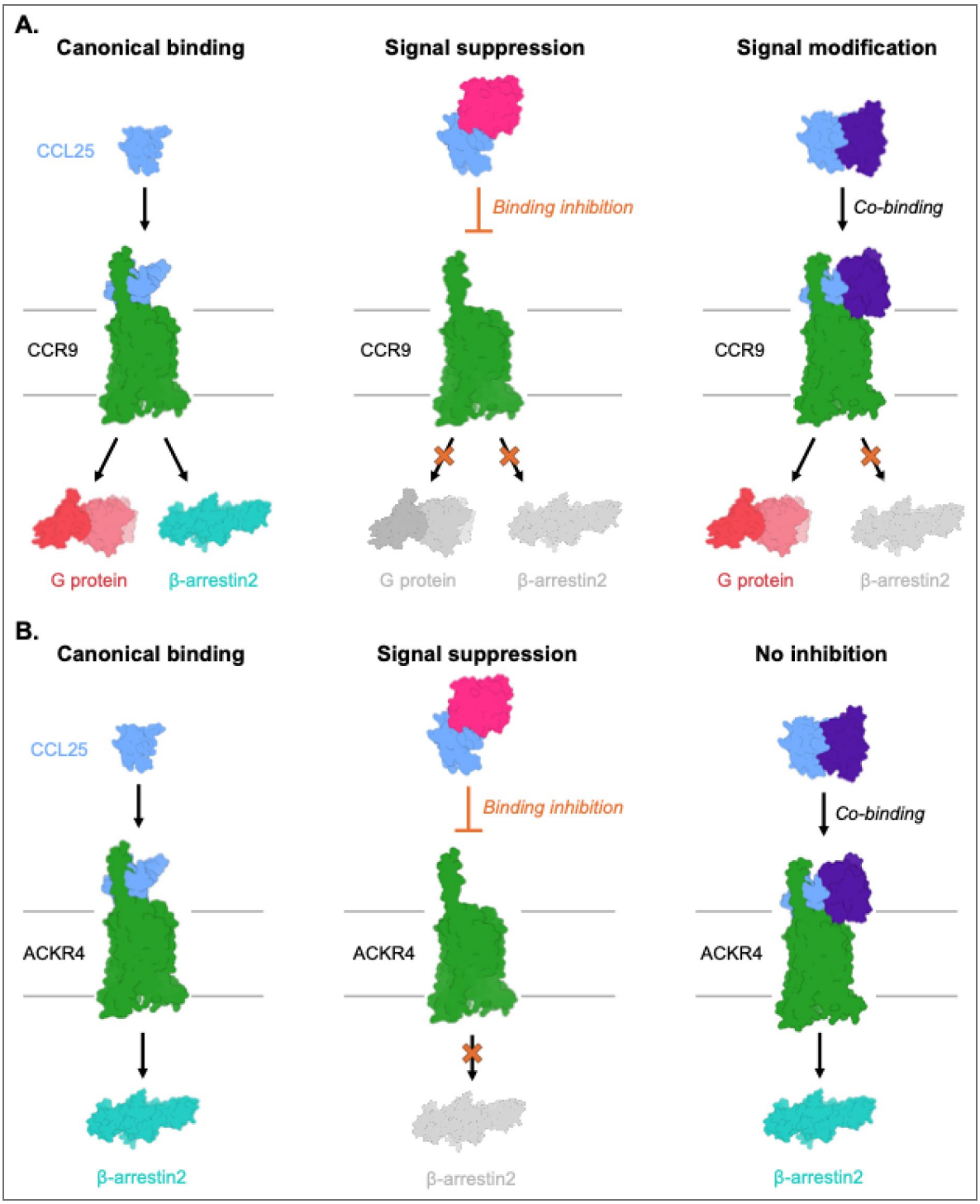


Figure 9. Mechanisms by which VUPs (VU miniproteins) modulate CCL25 signaling at CCR9 and ACKR4.

(**A**) Canonical engagement of CCL25 with CCR9 produces a balanced signaling response, activating both G protein- and β-arrestin2-dependent pathways. Signal suppression occurs when miniproteins (VUP25101, VUP25107, and VUP25112) sterically block CCL25:CCR9 interactions, leading to reduced activation of both G protein and β-arrestin2 signaling. Signal modification can also arise from co-binding of the CCL25:miniproteins complex to the receptor (VUP25111), resulting in biased signaling characterized by selective attenuation of the β-arrestin2 pathway while preserving G protein-mediated signaling for CCR9. (**B**) Canonical engagement of CCL25 with ACKR4 results in β-arrestin2 signaling. Signal suppression occurs when miniproteins (VUP25101, VUP25107, and VUP25112) sterically block CCL25:ACKR4 interactions, leading to reduced β-arrestin2 signaling. Miniprotein VUP25111 does not inhibit activation of ACKR4 by CCL25. The complex representing G protein is taken from PDB 9KO4 [45], the structure of β-arrestin2 was generated using AF3.

results (Fig. S7). Instead, the smaller residue showed exactly WT-like effector coupling in our experiments. The β1-binding interface of VUP25111 is similar to how CXC chemokine ligands, like CXCL12, dimerize. When the CXCL12 dimer binds its canonical receptor CXCR4, the second chemokine would also cause a large deflection of ECL2 of the receptor. Signaling of dimeric CXCL12 through CXCR4 is also biased completely towards G proteins, analogous to the effects of VUP25111 on CCL25 activation of CCR9 [51]. While G protein signaling was largely intact with dimeric CXCL12 activation of CXCR4, migration was eliminated, unlike what is shown here for CCR9. This suggests that different mechanisms of migration are likely present for the different receptors and different cell lines, and CCR9-mediated migration of MOLT-4 cells is exclusively dependent on G protein activation.

The miniproteins displayed varying degrees of chemokine selectivity among CCL25, CCL20, and CXCL12, including cross-reactivity for some designs. Given that only two additional chemokines were examined, these experiments provide an initial assessment of selectivity. As chemokine selectivity was not explicitly optimized during design, broader experimental profiling and negative-design strategies may be required to establish and improve miniprotein selectivity. Targeting chemokines is an evolutionarily efficient method to modulate immune responses. Atypical chemokine receptors scavenge chemokines to direct canonical receptor-mediated migration, whereas ticks and viruses target chemokines to suppress host immune responses. Here, this mechanism is exploited through de novo binder design, demonstrating the potential application of new AI methods to generate novel binders with new modalities. The miniproteins are valuable research tools to study chemokines and the receptor:chemokine signaling pathways and offer new options for drug discovery programs. These results provide a framework for therapeutically targeting difficult-to-modulate chemokine receptors and reveal unexpected mechanisms for signaling bias.

Materials and Methods

Unless otherwise stated, all materials and reagents were purchased from Melford or Sigma-Aldrich. Prolume purple was purchased from Nanolight Technologies (Prolume Ltd.). All miniprotein expression plasmids were synthesized by and purchased from Genscript. Full length CCL25-AZ488, CCL25_ΔCT-AZ647 (1-77), and CCL20 were purchased from Protein Foundry.

Generation of de novo binders

The three-dimensional structure of human CCL25 was retrieved from the AlphaFold Protein Structure Database [37]. To produce the mature form of the chemokine, the N-terminal signal sequence (M1-T23) was removed and residue numbering was reset to begin with Q1. Additionally, the C-terminus was truncated to L77 to focus the binders to the chemokine fold and yield a model of CCL25_ΔCT (1-77). Binder designs were generated with BindCraft [31] (version 1.5.0) using default_filters and the default_4stage_multimer protocol. Binders were allowed to have a length of between 75 and 125 amino acids. No hotspot residues were specified, thereby allowing the design algorithm to explore binding across the entire accessible surface of CCL25. In total, 101 designs were generated that passed computational filters and ranked using the ipTM score.

Comparison of structural similarity among binders was performed using the calculation of TM-scores using TM-align [52]. For each complex, the binder chain was extracted, and all pairwise combinations of generated binders were aligned using TM-align. To obtain a low-dimensional representation of structural relationships, TM-scores were converted to a distance matrix (1 – TM-score), and a two-dimensional embedding was generated using UMAP [53] (n_neighbors = 10, min_dist = 0.1, metric = “precomputed”).

Molecular interactions between the miniproteins designs and CCL25 were calculated with ProLIF [54] using the outputted structure from BindCraft.

Molecular dynamics simulations

Complexes from BindCraft were prepared using the CHARMM-GUI [55] solution builder. Protonation states of residues were assigned at pH 7.4 within the CHARMM-GUI solution builder. For terminal group patching, the N-terminus was acetylated (ACE patch), and the C-terminus was methylamidated (CT3 patch). The complexes were solvated in a cubic water box with a 10 Å buffer and neutralized to 0.15 M NaCl. The CHARMM36m force-field [56] parameters were used for the proteins and ions, while the TIP3P model was used for water.

All MD simulations were performed using GROMACS 2025.1 [57]. Systems were first minimized using a 5000-step steepest-descent minimization (≤5000 steps; convergence threshold 1000 kJ/mol/nm). Subsequently, the system was equilibrated according to the protocol generated by CHARMM-GUI. Systems were subjected to a 125-ps NVT run with a 1 fs time step and positional restraints on all protein heavy atoms (force constants: 400 kJ/mol/nm² for backbone atoms and 40 kJ/mol/nm² for side chains). Initial velocities were generated from a Maxwell-Boltzmann distribution at 310.15 K. Temperature was maintained at 310.15 K using the v-rescale thermostat [58]. Production simulations were run for 100 ns in the NPT ensemble. The v-rescale thermostat was used to maintain a temperature of 310.15 K, and the pressure was kept at 1 bar via semi-isotropic coupling to the c-rescale barostat [59] (τp = 5.0 ps, compressibility = 4.5*10-5 bar). Bond lengths of hydrogen covalent bonds were constrained using the LINCS algorithm. Long-range electrostatic interactions were calculated with the particle mesh Ewald method and the Verlet cutoff scheme with a 1.2 nm cutoff for both PME electrostatics and Lennard-Jones interactions, the latter using a force-switch modifier between 1.0 and 1.2 nm. Atomic positions were saved every 50 ps.

Trajectory analysis was performed using GROMACS and MDAnalysis [60]. For each system, backbone RMSD, binding-site RMSD, and all-atom RMSD were calculated. These were done with proper masking in MDAnalysis. Binding free energies were estimated using gmx_MMPBSA [61] with the MM-GBSA method (igb = 5, 0.15 M salt). For each trajectory, 1001 frames (sampled every 100 ps over a 100 ns simulation) were included.

AlphaFold3 structure prediction

The AlphaFold3 [62] server was used to predict the structures of CCL25 (CCL25-CT, 1-77) bound to CCR9 and ACKR4. Sequences of CCL25 (UniProt: O15444), CCR9 (UniProt: P51686), and ACKR4 (UniProt: Q9NPB9) were retrieved from UniProt [63]. For each complex, five models were generated using default settings, and the top-ranked model was selected for visualization.

DNA Constructs and site-directed mutagenesis

Human CCR9 (1-369) and ACKR4 (1-350) were cloned into a pcDNA3.1 expression vector either alone or followed by a C-terminal RlucII tag as described previously [41]. For receptor binding assays, hCCR9 and hACKR4 were cloned into a pcDNA5 expression vector, wherein the mammalian promotor was replaced with EF1a promotor, preceded by a N-terminal SNAP-tag. GFP10-β-arrestin2 (gifted from N. Heveker, Université de Montréal) [64], NES-Venus-mGs/i143 (mG_i) [42], and mCitrine-EPAC-Rluc (CAMYEL) [65,66] were described previously. Site-directed mutagenesis was performed using the Q5 mutation kit (NEB) and confirmed by sanger sequencing.

Chemokine purification from E. Coli

The chemokines CCL25 and CXCL12 were expressed and purified in *E.coli* following previously established protocols [41,67]. Briefly, codon optimized chemokine sequences containing the 8x histidine-tag and enterokinase cleavage site were cloned into a pET21 vector. The synthesized plasmid was transformed into *E.coli* BL21(DE3)pLysS cells and protein expression was triggered by Isopropyl-β-D-thiogalactopyranoside (IPTG) induction. Inclusion bodies containing the chemokines were harvested by sonication and solubilized in a buffer composed of 50 mM Tris, 6 M guanidine-HCl, and 300 mM NaCl at pH 8.0. Next, the solubilized protein was purified using a nickel-nitrotriacetic acid (Ni-NTA) affinity column, subsequently washed with 50 mM MES, 6 M

guanidine-HCl, 300 mM NaCl pH 6.0 and eluted with 50 mM acetate, 6 M guanidine-HCl, 300 mM NaCl pH 4.0. The elution fraction was refolded in 50 mM Tris, 700 mM arginine-HCl, 1 mM EDTA, 1 mM GSSG, 200 mM glutamine, 0.1% Triton-X (v/v) pH 7.5 by dropwise addition. After refolding, the protein was dialyzed in 20 mM Tris with 150 mM NaCl pH 8.0. The 8xHis-tag was removed using Enterokinase (New England Biolabs), and cleavage was confirmed by SDS-PAGE and LC-MS. The tag-free chemokine was further purified on a Ni-NTA column, washing with 50 mM Tris pH 8.0, and elution in 6 M guanidine-HCl using either 50 mM MES (pH 6.0) or 50 mM acetate (pH 4.0) in two separate fractions. Next, these fractions were purified by reverse-phage HPLC on a Gemini C18 110A column (Phenomenex) with a linear 5-95% acetonitrile gradient in 0.1% TFA (v/v). The final purified chemokines were validated by LC-MS, lyophilized, and stored at -80 °C.

VUP purification from E. Coli

Plasmids encoding VUP constructs, N-terminally preceded by a 6x histidine purification tag, were transformed into *E. coli* BL21(DE3)pLysS by standard heat-shock transformation and plated on LB agar containing kanamycin (100 ug/mL). A single colony of each construct was inoculated into 5-10 mL LB supplemented with kanamycin (100 ug/mL) and grown overnight at 37 °C while shaking (300 rpm) to generate starter culture. The following day, 1:25 dilutions of overnight culture were made into fresh LB containing kanamycin (100 ug/mL) and grown at 37 °C while shaking (300 rpm) until mid-log phase (OD600 ~ 0.6-0.8). Protein expression was induced by addition of IPTG to a final concentration of 1 mM, followed by incubation of cultures for 5-6 hour at 37 °C while shaking. Cell pellets were resuspended in TBS (50 mM Tris pH 7.4, 150 mM NaCl) supplemented with DNAseI (Thermo Fisher) and protease inhibitors (cOmplete, EDTA-free) and subsequently lysed by sonication. Centrifugation was repeated under the same conditions as described earlier. Imidazole was added to the supernatant for final concentration of 20 mM. Prior to applying the supernatant, Ni-NTA columns were equilibrated in TBS with 20 mM imidazole. The columns were washed with 5 column volumes of TBS containing 20 mM imidazole to remove non-specifically bound proteins. Lastly, VUPs were eluted with TBS containing 300 mM imidazole. All fractions were analyzed by SDS-PAGE to assess the purity of the protein. Eluted VUP fractions were concentrated using a 10 kDa spin filter and buffer-exchanged with 4 column volumes of TBS and stored at -80 °C. The isoelectric point of VUP25111 is near physiological pH, thus the protein was buffer exchanged to 50 mM MES pH 6.0 150 mM NaCl to improve solubility and stability for long term storage.

Chemokine-miniprotein complex formation by fluorescence polarization

Fluorescently tagged CCL25 (CCL25-AZ488; final concentration 15 nM) was mixed 1:1 with VUP binders prepared in TRIS buffer (50 mM, pH 7.7) supplemented with 0.05% Pluronic Acid (w/v) and dispensed into a black 384-well microplate (Greiner, F-bottom). VUP binder solutions began at 10 µM and were tested in a fourfold serial dilution series. Fluorescence polarization measurements were performed using a PHERAstar plate reader set at 25 °C. The fluorescently labeled chemokine CCL25-AZ488 was excited at 485 nm, and emission was detected at 520 nm. The target milli polarization (mP) value was set to 20 and calibrated using the positive control (CCL25-AZ488 (15 nM) in buffer alone). Polarization data was calculated according to the standard equation: $mP = 1000x\frac{I\parallel - G \cdot I\perp}{I\parallel + G \cdot I\perp}$

Where $I_{\parallel}$ and $I_{\perp}$ represent the fluorescence intensities measured parallel and perpendicular to the plane of polarized excitation light, respectively. The results of three independent assays were normalized to vehicle and highest response, as displayed.

Transfection of HEK293 Cells

HEK293T cells (ATCC) were cultured in Dulbecco's Modified Eagle's Medium (DMEM, Thermo Fisher Scientific) containing 1% penicillin (v/v) + streptomycin (Gibco), and 10% Fetal Bovine Serum (v/v) (FBS, Bodinco) kept at 37 °C with 5% CO_2 in a humidified environment. Cells were transfected with 2 µg DNA per 1 million cells using 6 ug polyethyleneimine (PEI, Polysciences Inc.)

in 150 mM NaCl. When less than 2 µg of plasmid DNA was used, the total DNA amount was adjusted to 2 µg with empty pcDNA3.1 vector. The DNA-PEI mixtures were incubated for 15 minutes at room temperature (RT). Cells were detached using trypsin/EDTA solution (Thermo Fischer Scientific) and resuspended in DMEM. Cells were counted and then added to the DNA-PEI mixture. Cells were seeded at 30k/well on a white 96-well plate (Greiner) and incubated for 48 hour before readout.

Inhibition of CCL25 binding to receptors by TR-FRET

To make SNAP-CCR9 or SNAP-ACKR4 membranes, HEK293T cells were transfected with 2 µg of SNAP-GPCR DNA per 2 million cells using OptiMEM (Gibco) and PEI as described above. After 48 hour, cells were harvested in PBS at 4 °C and subsequently centrifuged for 10 minutes at 1500 x g. Pelleted membranes were resuspended in 80 mM $NaPO_4$ + 0.05% Pluronic acid (membrane buffer) and homogenized by sonication. Next, cells were centrifuged at 22000 x g and resuspended in membrane buffer and labelled with 100 nM Tag-lite SNAP-Lumi4-Tb labeling reagent (Revvity) for 1 hour at 37 °C. To wash of free label, membranes were washed at least five times with membrane buffer. Membranes were homogenized again by sonication, snap frozen in liquid nitrogen, and stored at -80 °C. CCL25_ΔCT-AZ647 (20 nM) was incubated for 30 min at RT with increasing concentrations of the miniproteins. Next, the receptor suspension was homogenized by sonication before adding it to the readout plate (96 well half-area microplate, Greiner). The CCL25_ΔCT-AZ647+VUP mixture was added to the membranes and centrifuged at 150 x g for 3 min before incubation for 30 min at RT. TR-FRET ratio was quantified using a PHERAstar plate reader equipped with an optic module that excites at 337 nm and measures at 620 nm (Tb) and 665 nm (FRET signal) using 400 flashes per well. TR-FRET ratio was determined by dividing the FRET intensity by the Tb intensity using a ratio factor of 10000.

β-Arrestin2 recruitment by BRET

HEK293T cells were transfected with 50 ng receptor-RlucII and 1 µg GFP10-β-arrestin2 as described previously [41]. After 48 hour incubation, cells were rinsed once with PBS and kept in Hank's balanced salt solution (HBSS) supplemented with 0.1% bovine serum albumin (BSA; Fraction V; PanReac Applichem, w/v) (assay buffer). Next, 5 µM of Prolume Purple (Prolume Ltd.) was added and incubated for 5 minutes at 37 °C. Cells were then stimulated with increasing concentrations of either CCL25 or VUP binders that have been preincubated with 20 nM CCL25 for 30 min. A PHERAstar plate reader (BMG) was used to measure bioluminescence at 410-80 nm and 515-30 nm at 37 °C. Prior to generating dose-response curves, a kinetic response was measured to determine the time point corresponding to the maximal CCL25-induced response. Based on these measurements, a 5 min stimulation time was selected for CCR9 and a 40 min stimulation time for ACKR4. BRET values were determined as the ratio of red and blue luminescence (515-30/410-80). The results of three independent assays were normalized to the mock (no chemokine) and highest CCL25 concentration.

mG_i recruitment by BRET

HEK293T cells were transfected with 50 ng CCR9-RlucII and 250 ng Venus-mG_i as described previously [41]. After 48 hour incubation, cells were rinsed once with PBS and kept in assay buffer. Next, 5 µM of Coelenterazine-h (CTZ-h, Promega) was added to the cells and incubated for 5 minutes at 37 °C. Cells were then stimulated with increasing concentrations of CCL25 or VUP binders that have been preincubated with 20 nM CCL25 for 30 min. Luminescence was measured using a PHERAstar plate reader using the 475-30 nm and 535-30 nm filters. BRET values were determined as the ratio of red and blue luminescence (535-30/475-80) 20 min after CCL25 addition. The results of three independent assays were normalized to the mock (no chemokine) and highest CCL25 concentration.

cAMP measurement by BRET

HEK293T cells were transfected with 400 ng untagged CCR9 and 800 ng CAMYEL (cAMP sensor using YFP-Epac-Rluc) as described previously [41]. After 48 hour incubation, cells were rinsed once with PBS and kept in assay buffer. Next, 5 µM of Coelenterazine-h (CTZ-h, Prolume Ltd) was added to the cells and incubated for 5 minutes at 37 °C as described before. After, cAMP levels were amplified with 10 µM forskolin (FSK, Sigma-Aldrich) for 10 min. Cells were then stimulated with increasing concentrations of CCL25 or VUP binders that have been preincubated with 20 nM CCL25 for 30 min. Suppression of cAMP production was quantified by the ratio of red and blue luminescence (535-30/475-80) 5 min after CCL25 addition. The results of three independent assays were normalized to the mock (no chemokine) and highest CCL25 concentration.

GRK3 recruitment by BRET

HEK293T cells were transfected with 250 ng CCR9-mV and 50 ng GRK3-nLuc as described previously [41]. After 48 hour incubation, cells were rinsed once with PBS and kept in assay buffer. Next, 20 µM of CTZ-400A (Bld. Pharma.) was added and incubated for 5 minutes at 37 °C. Cells were then stimulated with increasing concentrations of either CCL25 or VUP binders that have been preincubated with 20 nM CCL25 for 30 min. A PHERAstar plate reader (BMG) was used to measure bioluminescence at 475-30 nm and 535-30 nm. BRET values were determined as the ratio of red and blue luminescence (535-30/475-80) 20 min after CCL25 addition. The results of three independent assays were normalized to the mock (no chemokine) and highest CCL25 concentration.

CCL25-mediated internalization by BRET

HEK293T cells were transfected with 50 ng CCR9-RlucII and 200 ng rGFP-CAAX as described previously [41]. After 48 hour incubation, cells were rinsed once with PBS and kept in assay buffer. Next, 5 µM of Prolume Purple (Prolume Ltd.) was added and incubated for 5 minutes at 37 °C. Cells were then stimulated with increasing concentrations of either CCL25 or VUP binders that have been preincubated with 20 nM CCL25 for 30 min. A PHERAstar plate reader (BMG) was used to measure bioluminescence at 410-80 nm and 515-30 nm. BRET values were determined as the ratio of red and blue luminescence (515-30/410-80) 20 min after CCL25 addition. The results of three independent assays were normalized to the mock (no chemokine) and highest CCL25 concentration.

Molt-4 cell migration quantified by flow cytometry

Transwell chemotaxis assays were performed using TC inserts for 24-well plates, 8 µm pore size (Sarstedt). MOLT-4 cells (ATCC) were collected by centrifugation at 125 x g for 5 min and subsequently resuspended in RPMI 1640 + 10% FBS (Gibco, v/v) at a density of 400k/ml. Next, 80k cells were added to the inserts and placed in the 24-well plate with either an increasing concentration of CCL25 or a fixed concentration of CCL25 (260 nM) together with 10 µM of miniprotein in the bottom chamber (pre-incubated for 30 min). The plate was then incubated for 2 hour at 37°C in a humidified atmosphere with 5% CO_2. After incubation, cells in bottom chamber were counted using a Guava easyCyte flow cytometer (Cytek) as three technical replicates. Data is presented as percentage of migrated cells relative to the initial number of cells in the insert.

Statisical analysis

All statistical analyses were performed using GraphPad Prism 10. Information regarding graphic representation, including the use of symbols, bar plots, and error bars, is provided in the corresponding figure legends. Unless otherwise indicated, scatter plots depict the mean values obtained from three independent experiments, each performed in either duplicate or triplicate. The statistical analysis of scatterplots was done using the extra sum-of-squares F test in Prism in reference to VUP25101. In bar plots, columns represent the overall mean across independent experiments, whereas the individual data points correspond to the mean value of each separate

experiment. Error bars indicate the standard deviation (SD). The statistical significance was assessed using Welch ANOVA followed by a Dunnett's T3 multiple comparisons test comparing to no VUP.

Data availability

All relevant data supporting this study are included in the article or source data files.

Additional information

Funding

This publication is part of the project TRANSLATION with file number OCENW.M.24.006 which is partly financed by the Dutch Research Council (NWO) under the grant [grant ID: *https://doi.org/10.61686/YKUZU08217*].

Funding

Funder	Grant reference number	Author
Nederlandse Organisatie voor Wetenschappelijk Onderzoek (NWO)	https://doi.org/10.61686/YKUZU08217	Christopher T Schafer

Author ORCID iDs

Bas de Boer: https://orcid.org/0009-0004-2024-4704
Thomas D Lamme: https://orcid.org/0009-0005-2168-9809
Christopher T Schafer: https://orcid.org/0000-0001-9907-295X

Additional files

Supplemental Information

References

[1] **Boldajipour B,** Mahabaleshwar H, Kardash E, Reichman-Fried M, Blaser H, Minina S, Wilson D, Xu Q, Raz E (2008) Control of Chemokine-Guided Cell Migration by Ligand Sequestration. *Cell* **132**:463-473 https://doi.org/10.1016/J.CELL.2007.12.034 | PubMed

[2] **Koelink PJ,** Overbeek SA, Braber S, De Kruijf P, Folkerts G, Smit MJ, Kraneveld AD (2012) Targeting chemokine receptors in chronic inflammatory diseases: An extensive review. *Pharmacol Ther* **133**:1-18 https://doi.org/10.1016/J.PHARMTHERA.2011.06.008 | PubMed

[3] **Szekanecz Z,** Koch AE (2015) Successes and failures of chemokine-pathway targeting in rheumatoid arthritis. *Nature Reviews Rheumatology* **12**:5-13 https://doi.org/10.1038/nrrheum.2015.157 | PubMed

[4] **O'Hayre M,** Salanga CL, Handel TM, Hamel DJ (2010) Emerging concepts and approaches for chemokine-receptor drug discovery. *Expert Opin Drug Discov* **5**:1109-1122 https://doi.org/10.1517/17460441.2010.525633 | PubMed

[5] **Dyer DP** (2020) Understanding the mechanisms that facilitate specificity, not redundancy, of chemokine-mediated leukocyte recruitment. *Immunology* **160**:336-344 https://doi.org/10.1111/imm.13200 | PubMed

[6] **Kufareva I,** Gustavsson M, Zheng Y, Stephens BS, Handel TM (2017) What Do Structures Tell Us About Chemokine Receptor Function and Antagonism?. *Annu. Rev. Biophys* **46**:175-198 https://doi.org/10.1146/annurev-biophys-051013-022942 | PubMed

[7] **Sonawani A,** Kharche S, Dasgupta D, Sengupta D (2022) Insights into the dynamic interactions at chemokine-receptor interfaces and mechanistic models of chemokine binding. *J. Struct. Biol* **214** https://doi.org/10.1016/J.JSB.2022.107877 | PubMed

[8] **Kayastha K,** Zhou Y, Brünle S (2024) Structural perspectives on chemokine receptors. *Biochem. Soc. Trans* **52**:1011 https://doi.org/10.1042/BST20230358 | PubMed

[9] **Gustavsson M,** Dyer DP, Zhao C, Handel TM (2019) Kinetics of CXCL12 binding to atypical chemokine receptor 3 reveal a role for the receptor N-terminus in chemokine binding. *Sci. Signal* **12** https://doi.org/10.1126/SCISIGNAL.AAW3657 | PubMed

[10] **Stephens BS,** Ngo T, Kufareva I, Handel TM (2020) Functional anatomy of the full-length CXCR4-CXCL12 complex systematically dissected by quantitative model-guided mutagenesis. *Sci. Signal* **13** https://doi.org/10.1126/scisignal.aay5024 | PubMed

[11] **Wescott MP,** Kufareva I, Paes C, Goodman JR, Thaker Y, Puffer BA, Berdougo E, Rucker JB, Handel TM, Doranz BJ (2016) Signal transmission through the CXC chemokine receptor 4 (CXCR4) transmembrane helices. *Proc. Natl. Acad. Sci. U. S. A* **113**:9928-9933 https://doi.org/10.1073/pnas.1601278113 | PubMed

[12] **Gustavsson M,** Wang L, Van Gils N, Stephens BS, Zhang P, Schall TJ, Yang S, Abagyan R, Chance MR, Kufareva I, *et al.* (2017) Structural basis of ligand interaction with atypical chemokine receptor 3. *Nature Communications* **8**:14135 https://doi.org/10.1038/ncomms14135 | PubMed

[13] **Papadakis KA,** Prehn J, Nelson V, Cheng L, Binder SW, Ponath PD, Andrew DP, Targan SR (2000) The Role of Thymus-Expressed Chemokine and Its Receptor CCR9 on Lymphocytes in the Regional Specialization of the Mucosal Immune System. *The Journal of Immunology* **165**:5069-5076 https://doi.org/10.4049/JIMMUNOL.165.9.5069 | PubMed

[14] **Zaballos A,** Gutiérrez J, Varona R, Ardavín C, Márquez G (1999) Cutting Edge: Identification of the Orphan Chemokine Receptor GPR-9-6 as CCR9, the Receptor for the Chemokine TECK. *The Journal of Immunology* **162**:5671-5675 https://doi.org/10.4049/JIMMUNOL.162.10.5671 | PubMed

[15] **Wurbel MA,** Malissen B, Campbell JJ (2006) Complex regulation of CCR9 at multiple discrete stages of T cell development. *Eur. J. Immunol* **36**:73-81 https://doi.org/10.1002/EJI.200535203 | PubMed

[16] **Uehara S,** Grinberg A, Farber JM, Love PE (2002) A role for CCR9 in T lymphocyte development and migration. *J. Immunol* **168**:2811-2819 https://doi.org/10.4049/JIMMUNOL.168.6.2811 | PubMed

[17] **Koenecke C,** Förster R (2009) CCR9 and inflammatory bowel disease. *Expert Opin Ther Targets* **13**:297-306 https://doi.org/10.1517/14728220902762928 | PubMed

[18] **Wu X,** Sun M, Yang Z, Lu C, Wang Q, Wang H, Deng C, Liu Y, Yang Y (2021) The Roles of CCR9/CCL25 in Inflammation and Inflammation-Associated Diseases. *Front. Cell Dev. Biol* **9** https://doi.org/10.3389/FCELL.2021.686548 | PubMed

[19] **Wendt E,** Keshav S (2015) CCR9 antagonism: potential in the treatment of Inflammatory Bowel Disease. *Clin. Exp. Gastroenterol* **8**:119 https://doi.org/10.2147/CEG.S48305 | PubMed

[20] **Letsch A,** Keilholz U, Schadendorf D, Assfalg G, Asemissen AM, Thiel E, Scheibenbogen C (2004) Functional CCR9 expression is associated with small intestinal metastasis. *J. Invest. Dermatol* **122**:685-690 https://doi.org/10.1111/J.0022-202X.2004.22315.X | PubMed

[21] **Feagan BG,** Sandborn WJ, D'Haens G, Lee SD, Allez M, Fedorak RN, Seidler U, Vermeire S, Lawrance IC, Maroney AC, *et al.* (2015) Randomised clinical trial: vercirnon, an oral CCR9 antagonist, vs. placebo as induction therapy in active Crohn's disease. *Aliment Pharmacol Ther* **42**:1170-1181 https://doi.org/10.1111/APT.13398 | PubMed

[22] **Alcami A,** Saraiva M (2009) Chemokine Binding Proteins Encoded by Pathogens. *Adv. Exp. Med. Biol* **666**:167-179 https://doi.org/10.1007/978-1-4419-1601-3_13 | PubMed

[23] **Bhusal RP,** Eaton JRO, Chowdhury ST, Power CA, Proudfoot AEI, Stone MJ, Bhattacharya S (2020) Evasins: Tick Salivary Proteins that Inhibit Mammalian Chemokines. *Trends Biochem. Sci* **45**:108-122 https://doi.org/10.1016/J.TIBS.2019.10.003 | PubMed

[24] **Nibbs RJB,** Graham GJ (2013) Immune regulation by atypical chemokine receptors. *Nature Reviews Immunology* **13**:815-829 https://doi.org/10.1038/nri3544 | PubMed

[25] **Gosling J,** Dairaghi DJ, Wang Y, Hanley M, Talbot D, Miao Z, Schall TJ (2000) Cutting Edge: Identification of a Novel Chemokine Receptor That Binds Dendritic Cell-and T Cell-Active Chemokines Including ELC, SLC, and TECK. *The Journal of Immunology* **164** https://doi.org/10.4049/JIMMUNOL.164.6.2851 | PubMed

[26] **Zhou AL,** Jensen DR, Peterson FC, Thomas MA, Schlimgen RR, Dwinell MB, Smith BC, Volkman BF (2023) Fragment-based drug discovery of small molecule ligands for the human chemokine CCL28. *SLAS Discovery* **28**:163-169 https://doi.org/10.1016/j.slasd.2023.02.004 | PubMed

[27] **Jumper J,** Evans R, Pritzel A, Green T, Figurnov M, Ronneberger O, Tunyasuvunakool K, Bates R, Žídek A, Potapenko A, *et al.* (2021) Highly accurate protein structure prediction with AlphaFold. *Nature* **596**:583-589 https://doi.org/10.1038/s41586-021-03819-2 | PubMed

[28] **Fox DR,** Taveneau C, Clement J, Grinter R, Knott GJ (2025) Code to complex: AI-driven de novo binder design. *Structure* **33**:1631-1642 https://doi.org/10.1016/j.str.2025.08.007 | PubMed

[29] **Team CD,** Boitreaud J, Dent J, Geisz D, McPartlon M, Meier J, Qiao Z, Rogozhnikov A, Rollins N, Wollenhaupt P, *et al.* (2025) Zero-shot antibody design in a 24-well plate. *BioRxiv* https://doi.org/10.1101/2025.07.05.663018

[30] **Zambaldi V,** La D, Chu AE, Patani H, Danson AE, Kwan TOC, Frerix T, Schneider RG, Saxton D, Thillaisundaram A, *et al.* (2024) De novo design of high-affinity protein binders with AlphaProteo. *arXiv* https://doi.org/10.48550/arxiv.2409.08022

[31] **Pacesa M,** Nickel L, Schellhaas C, Schmidt J, Pyatova E, Kissling L, Barendse P, Choudhury J, Kapoor S, Alcaraz-Serna A, *et al.* (2025) One-shot design of functional protein binders with BindCraft. *Nature* **646**:483-492 https://doi.org/10.1038/s41586-025-09429-6 | PubMed

[32] **Evans R,** O'Neill M, Pritzel A, Antropova N, Senior A, Green T, Žídek A, Bates R, Blackwell S, Yim J, *et al.* (2022) Protein complex prediction with AlphaFold-Multimer. *bioRxiv* https://doi.org/10.1101/2021.10.04.463034

[33] **Goverde CA,** Pacesa M, Goldbach N, Dornfeld LJ, Balbi PEM, Georgeon S, Rosset S, Kapoor S, Choudhury J, Dauparas J, *et al.* (2024) Computational design of soluble and functional membrane protein analogues. *Nature* **631**:449-458 https://doi.org/10.1038/s41586-024-07601-y | PubMed

[34] **Leman JK,** Weitzner BD, Lewis SM, Adolf-Bryfogle J, Alam N, Alford RF, Aprahamian M, Baker D, Barlow KA, Barth P, *et al.* (2020) Macromolecular modeling and design in Rosetta: recent methods and frameworks. *Nat. Methods* **17**:665-680 https://doi.org/10.1038/s41592-020-0848-2 | PubMed

[35] **Filius M,** Patsos T, Minnee H, Turco G, Chong HE, Liu J, Gnatzy M, Rooth RSM, Liu ACH, Ta RDT, *et al.* (2025) Evaluating BindCraft for Generative Design of High-Affinity Peptides. *ACS Chem. Biol* https://doi.org/10.1021/ACSCHEMBIO.5C00774 | PubMed

[36] **Smith EW,** Nevins AM, Qiao Z, Liu Y, Getschman AE, Vankayala SL, Kemp MT, Peterson FC, Li R, Volkman BF, *et al.* (2016) Structure-Based Identification of Novel Ligands Targeting Multiple Sites within a Chemokine–G-Protein-Coupled-Receptor Interface. *J. Med. Chem* **59**:4342-4351 https://doi.org/10.1021/ACS.JMEDCHEM.5B02042 | PubMed

[37] **Bertoni D,** Tsenkov M, Magana P, Nair S, Pidruchna I, Querino Lima Afonso M, Midlik A, Paramval U, Lawal D, Tanweer A, *et al.* (2013) AlphaFold Protein Structure Database 2025: a redesigned interface and updated structural coverage. *Nucleic Acids Res.* **1**:13-14 https://doi.org/10.1093/NAR/GKAF1226 | PubMed

[38] **Valdés-Tresanco MS,** Valdés-Tresanco ME, Valiente PA, Moreno E (2021) gmx_MMPBSA: A New Tool to Perform End-State Free Energy Calculations with GROMACS. *J. Chem. Theory Comput* **17**:6281-6291 https://doi.org/10.1021/ACS.JCTC.1C00645 | PubMed

[39] **Abramson J,** Adler J, Dunger J, Evans R, Green T, Pritzel A, Ronneberger O, Willmore L, Ballard AJ, Bambrick J, *et al.* (2024) Accurate structure prediction of biomolecular interactions with AlphaFold 3. *Nature* **630**:493-500 https://doi.org/10.1038/s41586-024-07487-w | PubMed

[40] **Watts AO,** Verkaar F, Van Der Lee MMC, Timmerman CAW, Kuijer M, Van Offenbeek J, Van Lith LHCJ, Smit MJ, Leurs R, Zaman GJR, *et al.* (2013) β-Arrestin Recruitment and G Protein Signaling by the Atypical Human Chemokine Decoy Receptor CCX-CKR. *Journal of Biological Chemistry* **288**:7169-7181

https://doi.org/10.1074/JBC.M112.406108 | PubMed

[41] **Lamme TD,** Smit MJ, Schafer CT (2025) Signal termination of the chemokine receptor CCR9 is governed by an arrestin-independent phosphorylation mechanism. *Journal of Biological Chemistry* **301** https://doi.org/10.1016/j.jbc.2025.108462 | PubMed

[42] **Wan Q,** Okashah N, Inoue A, Nehme R, Carpenter B, Tate CG, Lambert NA (2018) Mini G protein probes for active G protein-coupled receptors (GPCRs) in live cells. *J. Biol. Chem* **293**:7466-7473 https://doi.org/10.1074/JBC.RA118.001975 | PubMed

[43] **Namkung Y,** Le Gouill C, Lukashova V, Kobayashi H, Hogue M, Khoury E, Song M, Bouvier M, Laporte SA (2016) Monitoring G protein-coupled receptor and β-arrestin trafficking in live cells using enhanced bystander BRET. *Nat. Commun* **7** https://doi.org/10.1038/NCOMMS12178 | PubMed

[44] **Uhlen M,** Karlsson MJ, Zhong W, Tebani A, Pou C, Mikes J, Lakshmikanth T, Forsström B, Edfors F, Odeberg J, *et al.* (2019) A genome-wide transcriptomic analysis of protein-coding genes in human blood cells. *Science* **366** https://doi.org/10.1126/SCIENCE.AAX9198 | PubMed

[45] **Cao Y,** Zhang C, Yuan Q, Zhao F, Liu Q, Wu K, Hu W, He J, Li H, Xu HE, *et al.* (2025) Mechanisms of chemokine recognition and receptor activation of chemokine receptor CCR7. *Cell Rep* **44** https://doi.org/10.1016/J.CELREP.2025.116582 | PubMed

[46] **Bekker P,** Ebsworth K, Walters MJ, Berahovich RD, Ertl LS, Charvat TT, Punna S, Powers JP, Campbell JJ, Sullivan TJ, *et al.* (2015) CCR9 Antagonists in the Treatment of Ulcerative Colitis. *Mediators Inflamm* https://doi.org/10.1155/2015/628340 | PubMed

[47] **Zhang J,** Romero J, Chan A, Goss J, Stucka S, Cross J, Chamberlain B, Varoglu M, Chandonnet H, Ryan D, *et al.* (2015) Biarylsulfonamide CCR9 inhibitors for inflammatory bowel disease. *Bioorg Med Chem Lett* **25**:3661-3664 https://doi.org/10.1016/J.BMCL.2015.06.046 | PubMed

[48] **Anishchenko I,** Pellock SJ, Chidyausiku TM, Ramelot TA, Ovchinnikov S, Hao J, Bafna K, Norn C, Kang A, Bera AK, *et al.* (2021) De novo protein design by deep network hallucination. *Nature* **600**:547-552 https://doi.org/10.1038/s41586-021-04184-w | PubMed

[49] **Kortemme T** (2024) De novo protein design—From new structures to programmable functions. *Cell* **187**:526-544 https://doi.org/10.1016/J.CELL.2023.12.028 | PubMed

[50] **De Magalhaes Pinheiro I,** Dawson JRD, Calo N, Paolini-Bertrand M, Akondi KB, Tan G, Handel TM, Kufareva I, Hartley O (2025) Noncanonical roles of chemokine regions in CCR9 activation revealed by structural modeling and mutational mapping. *Nat. Commun* **16** https://doi.org/10.1038/s41467-025-62321-9 | PubMed

[51] **Drurya LJ,** Ziarek JJ, Gravel S, Veldkamp CT, Takekoshi T, Hwang ST, Heveker N, Volkman BF, Dwinell MB (2011) Monomeric and dimeric CXCL12 inhibit metastasis through distinct CXCR4 interactions and signaling pathways. *Proc. Natl. Acad. Sci. U. S. A* **108**:17655-17660 https://doi.org/10.1073/pnas.1101133108 | PubMed

[52] **Zhang Y,** Skolnick J (2005) TM-align: a protein structure alignment algorithm based on the TM-score. *Nucleic Acids Res* **33**:2302-2309 https://doi.org/10.1093/NAR/GKI524 | PubMed

[53] **McInnes L,** Healy J, Melville J (2018) UMAP: Uniform Manifold Approximation and Projection for Dimension Reduction. *arxiv* https://doi.org/10.48550/arXiv.1802.03426

[54] **Bouysset C,** Fiorucci S (2021) ProLIF: a library to encode molecular interactions as fingerprints. *Journal of Cheminformatics* **13**:72 https://doi.org/10.1186/S13321-021-00548-6 | PubMed

[55] **Lee J,** Cheng X, Swails JM, Yeom MS, Eastman PK, Lemkul JA, Wei S, Buckner J, Jeong JC, Qi Y, *et al.* (2015) CHARMM-GUI Input Generator for NAMD, GROMACS, AMBER, OpenMM, and CHARMM/OpenMM Simulations Using the CHARMM36 Additive Force Field. *J. Chem. Theory Comput.* **12**:405-413 https://doi.org/10.1021/ACS.JCTC.5B00935 | PubMed

[56] **Huang J,** Rauscher S, Nawrocki G, Ran T, Feig M, De Groot BL, Grubmüller H, MacKerell AD (2016) CHARMM36m: an improved force field for folded and intrinsically disordered proteins. *Nat. Methods* **14**:71-73 https://doi.org/10.1038/nmeth.4067 | PubMed

[57] **Van Der Spoel D,** Lindahl E, Hess B, Groenhof G, Mark AE, Berendsen HJC (2005) GROMACS: Fast, flexible, and free. *J. Comput. Chem.* **26**:1701-1718 https://doi.org/10.1002/jcc.20291 | PubMed

[58] **Bussi G,** Donadio D, Parrinello M (2007) Canonical sampling through velocity rescaling. *Journal of Chemical Physics* **126**:14101 https://doi.org/10.1063/1.2408420 | PubMed

[59] **Bernetti M,** Bussi G (2020) Pressure control using stochastic cell rescaling. *Journal of Chemical Physics* **153**:114107 https://doi.org/10.1063/5.0020514 | PubMed

[60] **Michaud-Agrawal N,** Denning EJ, Woolf TB, Beckstein O (2011) MDAnalysis: A toolkit for the analysis of molecular dynamics simulations. *J. Comput. Chem* **32**:2319-2327 https://doi.org/10.1002/JCC.21787 | PubMed

[61] **Valdés-Tresanco MS,** Valdés-Tresanco ME, Valiente PA, Moreno E (2021) gmx_MMPBSA: A New Tool to Perform End-State Free Energy Calculations with GROMACS. *J. Chem. Theory Comput* **17**:6281-6291 https://doi.org/10.1021/ACS.JCTC.1C00645 | PubMed

[62] **Abramson J,** Adler J, Dunger J, Evans R, Green T, Pritzel A, Ronneberger O, Willmore L, Ballard AJ, Bambrick J, *et al.* (2024) Accurate structure prediction of biomolecular interactions with AlphaFold 3. *Nature* **630**:493-500 https://doi.org/10.1038/s41586-024-07487-w | PubMed

[63] **Bateman A,** Martin MJ, Orchard S, Magrane M, Adesina A, Ahmad S, Bowler-Barnett EH, Bye-A-Jee H, Carpentier D, Denny P, *et al.* (2025) UniProt: the Universal Protein Knowledgebase in 2025. *Nucleic Acids Res* **53** https://doi.org/10.1093/NAR/GKAE1010 | PubMed

[64] **Schafer CT,** Chen Q, Tesmer JJG, Handel TM (2023) Atypical Chemokine Receptor 3 "Senses" CXC Chemokine Receptor 4 Activation Through GPCR Kinase Phosphorylation. *Mol. Pharmacol* **104**:174-186 https://doi.org/10.1124/MOLPHARM.123.000710 | PubMed

[65] **Hunter MR,** Finlay DB, Macdonald CE, Cawston EE, Grimsey NL, Glass M (2017) Real-Time Measurement of Cannabinoid Receptor-Mediated cAMP Signaling. *Methods Enzymol* **593**:43-59 https://doi.org/10.1016/BS.MIE.2017.05.001 | PubMed

[66] **Roy S,** Sinha S, Silas AJ, Ghassemian M, Kufareva I, Ghosh P (2024) Growth factor-dependent phosphorylation of Gαi shapes canonical signaling by G protein-coupled receptors. *Sci. Signal* **17** https://doi.org/10.1126/scisignal.ade8041 | PubMed

[67] **Gustavsson M,** Zheng Y, Handel TM (2016) Production of Chemokine/Chemokine Receptor Complexes for Structural Biophysical Studies. *Methods Enzymol* **570**:233-260 https://doi.org/10.1016/BS.MIE.2015.10.003 | PubMed

Peer reviews

Reviewer #1 (Public review):

Summary:

In this manuscript, the authors describe the use of BindCraft computational protein design to create a series of binders to the chemokine CCL25. This chemokine normally mediates CCR9-dependent trafficking of immune cells to the gut, making it a potential target for the treatment of inflammatory bowel disease and related conditions. Importantly, CCL25 also binds a scavenging receptor, ACKR4. The computational protein design approach used does not involve defining particular epitopes to be targeted, allowing a free search for any potential interaction surface.

Among four designs tested, three were predicted to interact at a similar site on the chemokine, while a fourth clone, VUP25111, was predicted to bind to a different site. All four designs showed binding to CCL25, with similar high-nM KD values in all cases. The first three clones showed evidence of direct competition with the receptor for CCL25 binding, while VUP25111 showed incomplete inhibition of binding. In functional assays, all clones acted as antagonists except for VUP25111, which inhibited arrestin recruitment by CCR9, but did not

affect G protein activation by CCR9 or arrestin recruitment by ACKR4 (which signals exclusively through arrestin and not G protein).

Strengths:

The work is completed to a high technical standard, and the functional diversity of the clones is intriguing. It is exciting to see pathway-selective modulation of signaling, and this basic paradigm is likely to generalize to other chemokine/receptor systems. The exceptional complexity of chemokine signaling makes this an excellent area to explore the development of modulators that can restrict signaling to a specific subset of receptors.

Weaknesses:

No major weaknesses were noted by this reviewer.

Comments on revised version:

The revision looks fine to me.

https://doi.org/10.7554/eLife.111190.2.sa3

Reviewer #2 (Public review):

This study from de Boer, Lamme, Verdwaald and Schafer describes the de novo AI-guided design of miniproteins that target the chemokine CCL25, with the aim to modulate the activation and signalling of the chemokine receptors CCR9 and ACKR4. The study focuses on characterising four miniproteins that all bind CCL25 with good affinity. Three designs appear to prevent CCL25 binding to both CCR9 and ACKR4, with increasing concentrations of miniproteins resulting in decreased arrestin (both receptors) and mini G protein recruitment (CCR9), less inhibition of forskolin-stimulated cAMP (CCR9), and decreased GRK3 recruitment and receptor internalisation (CCR9). One miniprotein, VUP25111, changes the properties of CCL25 rather than preventing ligand/receptor interactions, resulting in greater selectivity for CCR9 over ACKR4 and a G protein-biased signalling profile (maintenance of mini G protein recruitment, GRK3 recruitment, inhibition of cAMP and receptor internalisation, but loss of arrestin recruitment). VUP25111 also maintained chemotactic migration in MOLT-4 T lymphoblast cells, whereas this response was lost in the presence of the other three miniproteins.

Overall, this is a very interesting application of AI-designed de novo miniproteins to modulate GPCR responses by directly binding the ligand rather than the receptor. This is a conceptually very intriguing approach that could, in principle, be extended to other GPCR systems beyond the chemokine family. The authors deploy an impressive array of assays spanning multiple signalling endpoints, providing a thorough picture of how each miniprotein influences receptor activation and downstream signalling. The presentation of concentration-response relationships for CCL25 alone and in the presence of each miniprotein is particularly informative, and the figures are very well constructed throughout. The inclusion of clear cartoons illustrating the basis of each assay is a nice touch that will help readers from outside the immediate field follow the logic of each experiment.

https://doi.org/10.7554/eLife.111190.2.sa2

Reviewer #3 (Public review):

The authors employed the BindCraft platform to develop binders targeting the chemokine CCL25, a selective activator of the chemokine receptor CCR9. They successfully generated two classes of binders: one that inhibits all CCL25-mediated CCR9 activation, and another that

permits CCR9 G protein signaling while simultaneously preventing arrestin recruitment. These tools will enable the dissection of arrestin involvement in regulating cell migration.

https://doi.org/10.7554/eLife.111190.2.sa1

Author response:

The following is the authors' response to the original reviews.

> ***Reviewer #1 (Public review):***
>
> *Summary:*
>
> *In this manuscript, the authors describe the use of BindCraft computational protein design to create a series of binders to the chemokine CCL25. This chemokine normally mediates CCR9-dependent trafficking of immune cells to the gut, making it a potential target for the treatment of inflammatory bowel disease and related conditions. Importantly, CCL25 also binds a scavenging receptor, ACKR4. The computational protein design approach used does not involve defining particular epitopes to be targeted, allowing a free search for any potential interaction surface.*
>
> *Among four designs tested, three were predicted to interact at a similar site on the chemokine, while a fourth clone, VUP25111, was predicted to bind to a different site. All four designs showed binding to CCL25, with similar high-nM KD values in all cases. The first three clones showed evidence of direct competition with the receptor for CCL25 binding, while VUP25111 showed incomplete inhibition of binding. In functional assays, all clones acted as antagonists except for VUP25111, which inhibited arrestin recruitment by CCR9, but did not affect G protein activation by CCR9 or arrestin recruitment by ACKR4 (which signals exclusively through arrestin and not G protein).*
>
> *Strengths:*
>
> *The work is completed to a high technical standard, and the functional diversity of the clones is intriguing. It is exciting to see pathway-selective modulation of signaling, and this basic paradigm is likely to generalize to other chemokine/receptor systems. The exceptional complexity of chemokine signaling makes this an excellent area to explore the development of modulators that can restrict signaling to a specific subset of receptors.*
>
> *Weaknesses:*
>
> *No major weaknesses were noted by this reviewer.*

We thank the reviewer for their positive response and thorough evaluation of our work. Below, we address their recommendations in detail in the private review.

> ***Reviewer #1 (Recommendations for the authors):***
>
> *Minor points for potential improvement:*
>
> *(1) Consider shortening the discussion section, which could benefit from a more focused discussion of the key conclusions and their implications. As written, it is rather long, and parts of it repeat material already covered elsewhere (e.g., the two-step binding mechanism is described in lines 55-64 and again in 331-335).*

We thank the reviewer for the suggestion to make the discussion more focused. We agree that parts repeat material from the introduction. As such, we have revised the discussion to

reduce repetition with the introduction, including removal of the repeated description of the two-step binding mechanism, and condensing several passages.

> *(2) The figures are clear, but it may be helpful to combine panels into a smaller number of figures to make direct comparisons among signaling curves more straightforward.*

We thank the reviewer for the suggestion to reduce the number of figures for easier curve comparisons. We prefer our current presentation of the figures so as not to conflate disparate themes and concepts; for example, GRK recruitment is a distinct event from receptor internalization. The pharmacological results have been compiled in Figure S8 in the supplementary to allow visual, side-by-side comparisons of the DRCs presented in the publication.

> ***Reviewer #2 (Public review):***
>
> *This study from de Boer, Lamme, Verdwaald and Schafer describes the de novo AI-guided design of miniproteins that target the chemokine CCL25, with the aim to modulate the activation and signalling of the chemokine receptors CCR9 and ACKR4. The study focuses on characterising four miniproteins that all bind CCL25 with good affinity. Three designs appear to prevent CCL25 binding to both CCR9 and ACKR4, with increasing concentrations of miniproteins resulting in decreased arrestin (both receptors) and mini G protein recruitment (CCR9), less inhibition of forskolin-stimulated cAMP (CCR9), and decreased GRK3 recruitment and receptor internalisation (CCR9). One miniprotein, VUP25111, changes the properties of CCL25 rather than preventing ligand/receptor interactions, resulting in greater selectivity for CCR9 over ACKR4 and a G protein-biased signalling profile (maintenance of mini G protein recruitment, GRK3 recruitment, inhibition of cAMP and receptor internalisation, but loss of arrestin recruitment). VUP25111 also maintained chemotactic migration in MOLT-4 T lymphoblast cells, whereas this response was lost in the presence of the other three miniproteins.*
>
> *Overall, this is a very interesting application of AI-designed de novo miniproteins to modulate GPCR responses by directly binding the ligand rather than the receptor. This is a conceptually very intriguing approach that could, in principle, be extended to other GPCR systems beyond the chemokine family. The authors deploy an impressive array of assays spanning multiple signalling endpoints, providing a thorough picture of how each miniprotein influences receptor activation and downstream signalling. The presentation of concentration-response relationships for CCL25 alone and in the presence of each miniprotein is particularly informative, and the figures are very well constructed throughout. The inclusion of clear cartoons illustrating the basis of each assay is a nice touch that will help readers from outside the immediate field follow the logic of each experiment.*
>
> *There are two main conclusions that are not currently as well-supported by the evidence as they might be, and that would benefit from some qualification. The first concerns the selectivity of the miniproteins for CCL25. Testing the impact of the miniproteins on CXCL12 activation of CXCR4 is an important and welcome experiment, but it addresses selectivity against only one other chemokine system, and the current claim of specificity is therefore stronger than the data allow. Additionally, at the highest concentration tested (10 μM), the more potent miniproteins (VUP25101, VUP25107) appear to show some inhibition of arrestin recruitment to CXCR4 - perhaps unsurprising given the degree of structural conservation among chemokines. The statements regarding selectivity and the lack of effect on the CXCL12/CXCR4 system would benefit from revision to more accurately reflect these observations.*

We thank the reviewer for the detailed review and suggestions for our publication. We agree with the reviewer that testing against only one additional chemokine receptor: chemokine

pair is insufficient to support strong claims of selectivity. To further assess the selectivity of the miniproteins, we evaluated the effects of the VUPs against CCL20, a chemokine closely related to CCL25. CCL20 binds both CCR6 and ACKR4, providing an optimal platform to compare the effects on this non-specified target. Receptor activation was determined by β-arrestin recruitment (Fig. S6). For ACKR4, VUP25107 and VUP25112 have similar IC50 values for CCL20 and CCL25. In contrast, VUP25101 showed reduced potency towards CCL20 relative to CCL25 (CCL20 pIC50 = 6.06 ± 0.13, CCL25 pIC50 = 7.73 ± 0.08), suggesting greater selectivity. VUP25111 had no impact on activation of ACKR4 by CCL20, which may reflect a lack of engagement with the other chemokine or that it binds in a similar way as to CCL25 and does not impact chemokine-promoted ACKR4 activation. CCL20-mediated activation of CCR6 further supports the specificity of VUP25101, which showed only a modest effect at the highest concentration tested. In contrast, VUP25107 and VUP25112 showed a dose-dependent inhibition of arrestin recruitment ($pIC50_{VUP25107}$ = 6.99 ± 0.15, $pIC50_{VUP25112}$ = 7.49 ± 0.07).

We agree that a reduction in β-arrestin recruitment to CXCR4 is apparent at the highest concentration tested (10 μM) for VUP25101 and VUP25107. To further address the selectivity of these miniproteins, we have included β-arrestin recruitment data for ACKR3 (Fig. S5), the other chemokine receptor that binds CXCL12. A similar suppression was observed for the atypical receptor as for CXCR4 at the highest concentrations, suggesting cross-reactivity at high concentrations.

Based on the CCL20 and CXCL12 data, we have revised the text to more accurately reflect these observations. We now frame these results as an initial proof of concept demonstrating the feasibility of this design approach, while noting that further optimization and characterization of selectivity will be required to advance the miniproteins for additional applications.

To reflect this, we have added the following text on Pg.9:

“CCL25 specificity was experimentally evaluated by testing the miniproteins against CXCL12 by tracking arrestin recruitment to CXCR4 and ACKR3, the native agonist for this canonical and atypical receptor pair (Fig. S5). VUP25111 and VUP25112 showed no effect on CXCL12-mediated activation at any concentration, while VUP25101 and VUP25107 showed partial inhibition at the highest tested concentration (10 μM).

In addition, the effects of the VUPs were evaluated against CCL20, a closely related chemokine to CCL25, by assessing arrestin recruitment to CCR6 and ACKR4 (Fig. S6). VUP25107 and VUP25112 displayed similar inhibitory potencies of CCL20 as to CCL25 for ACKR4 (VUP25107: pIC50 = 7.72 ± 0.21; VUP25112: pIC50 = 6.93 ± 1.03). In contrast, VUP25101 showed reduced inhibition of CCL20 relative to CCL25 (VUP25101: $pIC50_{CCL20}$ = 6.06 ± 0.13 v $pIC50_{CCL25}$ = 7.73 ± 0.08), indicating greater selectivity for the designed target. CCL20 activation of CCR6 further supports the specificity of VUP25101, which only showed a modest effect at the highest concentration tested. VUP25111 showed no inhibitory effects on CCL20 activation of either CCR6 nor ACKR4, which may indicate a lack of binding, but is also indiscernible from forming a receptor-competent complex similar to the proposed CCL25:VUP25111:ACKR4 interaction.”

And added the following in the discussion on Pg.15:

“The miniproteins displayed varying degrees of chemokine selectivity among CCL25, CCL20, and CXCL12, including cross-reactivity for some designs. Given that only two additional chemokines were examined, these experiments provide an initial assessment of selectivity. As chemokine selectivity was not explicitly optimized during design, broader experimental profiling and negative-design strategies may be required to establish and improve miniprotein selectivity.”

> *The second concern relates to the interpretation of the preserved GRK3 recruitment, but*

> *the complete loss of arrestin recruitment observed with VUP25111. In the GRK3 recruitment experiments, 20 nM CCL25 was used, representing an EC40 concentration in this assay. VUP25111 causes a concentration-dependent reduction in CCL25-induced GRK3 recruitment, down to approximately 15% of the maximal response. It is worth considering whether this degree of reduction in GRK3 recruitment could itself be sufficient to disrupt patterns of receptor phosphorylation and thereby prevent observable arrestin recruitment. Both interpretations are complicated by the fact that the GRK3 recruitment and arrestin recruitment assays likely differ in their sensitivity and dynamic windows, making direct quantitative comparisons between them difficult. In the absence of direct measurements of CCR9 phosphorylation in the presence of VUP25111, the alternative interpretation remains open and would benefit from acknowledgement. Given recent work from the same group demonstrating that receptor internalisation is only partially dependent on arrestins (Lamme et al., 2025, J Biol Chem), further discussion of the relationship between GRK and arrestin recruitment and CCR9 internalisation would be of value to the broader GPCR audience this work is likely to attract.*

We appreciate the reviewer's careful analysis of our results and highlighting earlier work from our group. The reviewer is correct that the discrepancy between VUP25111's impact on GRK3 and arrestin recruitment can also be explained by the decrease in GRK3 recruitment reflecting a sufficient change in receptor phosphorylation to account for the loss of arrestin engagement and not solely by the presented interpretation of the adoption of an arrestin-incompatible conformation with retained phosphorylation. The main text has been modified on pg. 11 to reflect this potential:

"This suggests that either activation of CCR9 by the VUP25111:CCL25 complex promotes a conformation incompatible with arrestin engagement, but still accessible for GRK phosphorylation, or the reduced GRK interaction represents the formation of a phosphorylation barcode incapable of supporting arrestin recruitment. Without direct phosphorylation measurements these possibilities cannot be separated."

And in the discussion on pg.14:

"The extent of phosphorylation is not clear, and the inhibited GRK recruitment may reflect the formation of sub-phosphorylated states which cannot support arrestin recruitment nor promote efficient receptor internalization. Alternatively, the miniprotein: chemokine complex may induce a conformational state incompatible with arrestin engagement."

A partial phosphorylation explanation has also been added on internalization on pg.12:

"These results suggest that the VUP25111:CCL25 complex suppresses both the arrestin-dependent and independent internalization mechanisms used by CCR9, despite likely allowing for some, albeit perhaps insufficient, GRK phosphorylation."

> *Finally, some additional justification for the use of 20 nM CCL25 across all assays would strengthen the study, as this concentration represents different points on the concentration-response curve depending on the assay and receptor in question. It ranges from an EC40 for CCR9 GRK3 recruitment and internalisation, to an EC50 for CCR9 arrestin and mini-Gi recruitment, an EC80 for CCR9 cAMP inhibition, and an Emax for ACKR4 arrestin recruitment. This has potential consequences for the interpretation and cross-assay comparison of miniprotein potency, and the authors are encouraged to acknowledge and discuss this in the context of their conclusions.*

We thank the reviewer for highlighting the need to discuss CCL25 concentration across assays. Our primary aim was to use a single CCL25 concentration to enable direct comparison of all assay outcomes against the same CCL25:miniproteins ratio, since the miniproteins are

designed to antagonize the chemokine, rather than the receptor. We set the concentration at 20 nM based on the first arrestin recruitment assays to CCR9, where we initially characterized miniprotein: CCL25 activity. Importantly, CCL25 has lower potency for CCR9 than ACKR4, making it the limiting case. Selecting 20 nM ensured responses within the EC40-EC80 range for all assays. To improve clarity, we have now explicitly stated this rationale in the manuscript and noted the implications of using a single CCL25 concentration across diverse readouts on Pg.10:

"Despite the higher potency of CCL25 for cAMP inhibition compared to arrestin recruitment, a fixed concentration of 20 nM CCL25 was used throughout this and subsequent assays to maintain a consistent CCL25:miniprotein stoichiometry. As this concentration represents different points on the respective concentration-response curves, cross-assay comparisons of apparent miniprotein potency should be interpreted qualitatively."

> ***Reviewer #2 (Recommendations for the authors):***
>
> *Major points:*
>
> *(1) The conclusions regarding miniprotein selectivity for CCL25 would benefit from revision to reflect that only the CXCL12/CXCR4 system was tested as a counter-screen. The apparent inhibition of arrestin recruitment to CXCR4 by VUP25101 and VUP25107 at 10 μM should be acknowledged/discussed.*

We thank the reviewer for this comment and agree that selectivity should be more explicitly acknowledged. This point has been thoroughly addressed in our response in the public review. Briefly, we have added a similar selectivity assay but now against CCL20, which is closely related to CCL25, as well as revisiting the CXCL12 assay with ACKR3 that was originally presented in the manuscript. Statements in the text have been added to note the apparent inhibition at 10 μM for VUP25101 and VUP25107.

> *(2) The conclusions regarding G protein-biased signalling driven by VUP25111 would benefit from qualification. In particular, it is worth acknowledging that a substantial reduction in GRK3 recruitment may itself be sufficient to account for the observed loss of arrestin recruitment, and that direct measurement of CCR9 phosphorylation in the presence of VUP25111 would help to resolve this. Discussion of the relationship between GRK recruitment, receptor phosphorylation, arrestin recruitment and internalisation in this context would also be of value to the broader GPCR audience this work is likely to attract.*

We agree with the reviewer that an incomplete or insufficient level of phosphorylation could also explain our arrestin and internalization results presented by the VUP25111:CCL25 complex. We have added the following to the discussion on pg. 14 and modified the results to better reflect the multiple interpretations:

"The extent of phosphorylation is not clear and the inhibited GRK recruitment may reflect the formation of sub-phosphorylated states which cannot support arrestin recruitment, nor promote efficient receptor internalization. Alternatively, the complete inhibition of arrestin engagement cannot be easily explained by phosphorylation, and instead suggests the miniprotein: chemokine complex may induce a conformational state incompatible with arrestin engagement. Due to the clash with ECL2, the loop would need to distort to accommodate the larger ligand complex and this displacement may translate into the G protein and GRK-permissive structural state."

> *(3) The choice of 20 nM CCL25 across assays should be justified or its implications discussed, particularly given that this concentration represents different effective concentrations for each endpoint and receptor.*

The rationale for using a fixed 20nM CCL25 concentration and its implications is now discussed within the main text as well as our response in the public review.

> *Modelling:*
>
> *Modelling of VUP25111 and VUP25101 binding to CCL25/receptor complexes is presented. Was the same analysis performed for VUP25112 and VUP25107, and do they similarly appear to interfere with direct receptor binding?*

We initially selected VUP25101 as a representative for VUP25112 and VUP25107 to simplify visualization. We have now extended the same modeling analysis to VUP25107 and VUP25112. These additional analyses have now been included in the revised manuscript in Fig. 3D.

> *Methods:*
>
> *(1) Percentage concentrations throughout the methods are missing w/v or v/v designations.*

We thank the reviewer for their careful reading and apologize for the oversight. We have added all w/v or v/v designations in the methods.

> *(2) More specific information for each BRET experiment would be useful. For example, incubation times with CCL25 and miniproteins (included for some but not all assays), and clarification of whether experiments were endpoint reads or timecourse experiments.*

We agree with the reviewer that the methods section could be clarified, as well as removing a lot of repetition. We have revised the methods.

> *Specific text revisions:*
>
> *(1) Abstract, line 20: "Most drug discovery efforts target the receptors, whereas natural regulatory mechanisms focus on the chemokines". This is unclear for a non-chemokine audience without additional context clarifying that this refers to binding to or modification of the chemokine itself to modulate receptor activation.*

To clarify this distinction for a broader readership, we revised the abstract to state explicitly that natural regulatory mechanisms modulate immune responses by directly binding to or modifying chemokines, thereby altering their ability to bind receptors. We have changed the text in the abstract on Pg.2 to:

“Most drug discovery efforts target the receptors, whereas natural regulatory mechanisms modulate immune responses by directly binding to or modifying the chemokine ligands.”

> *(2) Results, line 177: "In the case of VUP25111, only the highest tested concentrations decreased CCL25 binding to either receptor, but did not completely eliminate the binding signal". This should be revised as there is a clear concentration-dependent effect of VUP25111 on CCL25 binding.*

We have revised the text to reflect that VUP25111 inhibits CCL25 binding in a concentration-dependent manner, while also making clear that this inhibition occurs with significantly lower potency than the other miniproteins. We have changed the following text on Pg.7:

“VUP25111 shows a drastically lower inhibitory potency compared to the other binders and did not completely eliminate the binding signal.”

> *(3) Line 179: "...this suggests that CCL25:VUP25111 may bind the receptors cooperatively". Please revise; the meaning is unclear.*

Our results indicate that VUP25111 does not prevent CCL25 from engaging either receptor. To avoid ambiguity, we have revised the text to explicitly state that our results are consistent with the binding of a pre-formed VUP25111:CCL25 complex to the receptor, resulting in the formation of a VUP25111:CCL25:receptor complex. We have changed the following text on Pg.7:

“Since the binder readily complexes with the chemokine at these concentrations (Fig. 2), this suggests that the CCL25:VUP25111 complex retains the ability to bind the receptor.”

> *(4) Line 216: "VUP25112 also completely impaired CCL25-mediated activation of the atypical receptor at the highest concentrations, but with significantly less potency". Please provide statistical tests to support this statement.*

We thank the reviewer for requesting clarification regarding the statistical support for this statement. Statistical analyses supporting the conclusions in line 216, as well as other figures, were included in the initial manuscript but were provided in the supplementary information. To improve clarity in the manuscript, we have added explicit references to the corresponding supplementary statistical table in the text, added appropriate significance indicators to the relevant figures, and expanded the figure legends to state the statistical test used.

> *(5) Line 219: "The unique binder VUP25111, on the other hand, did not inhibit the activation of ACKR4 by CCL25 at any tested concentration". Please rephrase. While there was no concentration-dependent inhibition of arrestin recruitment to ACKR4, the addition of VUP25111 at any concentration appeared to reduce total arrestin recruitment to approximately 80% of the CCL25-alone condition.*

We would like to thank the reviewer for this careful analysis of the data. Although this may appear to be the case in the figure, there is no significant difference between the lowest concentration (2.5 nM) and vehicle condition (∞) for any miniprotein and no real difference can be claimed.

We have specifically noted this on Pg. 9:

“The unique binder VUP25111, on the other hand, did not significantly impact the activation of ACKR4 by CCL25 at any tested miniprotein concentration.”

> *(6) Line 240: "suggest that the specific ligand interactions driving arrestin engagement with CCR9 may be more strict than for the G proteins". An alternative interpretation is that the miniprotein specifically impairs the receptor conformation important for arrestin engagement, without affecting the conformation required for G protein engagement, and this should be acknowledged.*

We agree with the reviewer that these statements would benefit from further clarification. Indeed, the observed effects may not be only due to specific ligand interactions but could also depend on specific receptor conformations required for the specific protein-protein interactions. We have adjusted the following text on Pg.10:

“The deviations between the arrestin results (Fig. 4) and G protein (Fig. 5B) suggest that the specific ligand interactions or receptor conformations driving arrestin engagement with CCR9 may be more strict than for the G proteins.”

> ***Reviewer #3 (Public review):***
>
> *Summary:*
>
> *The authors employed the BindCraft platform to develop binders targeting the chemokine CCL25, a selective activator of the chemokine receptor CCR9. They successfully*

> *generated two classes of binders: one that inhibits all CCL25-mediated CCR9 activation, and another that permits CCR9 G protein signaling while simultaneously preventing arrestin recruitment. These tools will enable the dissection of arrestin involvement in regulating cell migration.*
>
> *My comments, in the order of reading:*
>
> *(1) Title: I strongly recommend removing the term "biasing" from the title. In this context, it does not convey a specific mechanistic concept. The term "biased signaling" has been used for a very broad range of mechanistically distinct pharmacological phenomena, and without a precise definition, it adds more confusion than clarity. I therefore suggest refraining from using it in the title.*

We appreciate the reviewer's concern regarding the use of the term "biasing" given its broad and sometimes ambiguous use in the literature. Most commonly it refers to G protein versus arrestin-mediated signalling but is also used in regard to GRK specificity as well as to discrete differences in receptor trafficking (Motso et al. 2025, Cell). In our study, we use this in a specific mechanistic sense, referring to the bias VUP25111 induces upon binding CCL25. The miniprotein: CCL25 complex inhibits CCR9 arrestin recruitment, receptor internalization, and GRK3 engagement while not affecting G protein recruitment (mGi), G protein-mediated signaling (CAMYEL), and cell migration. We compare these directly to the effects of the chemokine alone, which shows robust responses across all of these receptor outputs. The use of the term "biasing" in the title is reflective of this observed change in receptor response to the modified agonist. Additionally, as noted by the reviewer below, we compare similar outputs to compare the impact on effector coupling, eg. Arrestin and mini-G protein recruitment. We strongly feel that the term "biasing" most accurately describes the phenomenon we are describing with regard to the altered receptor response to the VUP25111:CCL25 complex and thus prefer to keep the title without alteration.

> *(2) Abstract, line 34: The term "bias" should be replaced. As currently used, it appears to suggest a dichotomy between G protein signaling and arrestin recruitment. However, arrestin recruitment is a consequence of G protein signaling, and it is not conceptually sound to compare a signaling event mediated by one protein family with a protein-protein interaction involving another protein family. A meaningful comparison requires experimental paradigms that differ by a single variable; in this case, there are two - distinct protein families and fundamentally different types of readouts (signaling versus protein-protein interaction).*

We agree that the term "bias" must be used with precision. One point of clarification, arrestin recruitment is not explicitly a consequence of G protein signaling. The atypical chemokine receptors, of which ACKR4 is a member, are well-established examples of GPCRs that do not bind nor activate G proteins yet still recruit arrestins (Lamme et al., 2026). While biased responses within the GPCR system are often the comparison of different events as noted by the reviewer, we compare the effects of miniproteins on the recruitment of mGi and arrestin via a BRET-based assay that assesses the direct protein: protein interactions between the receptor and effector. The lack of effect on mGi recruitment was further supported by measuring the effect of the miniproteins on downstream cAMP levels. To avoid any misunderstanding, we have revised the abstract to explicitly state that the observed effect induced by VUP25111 is evaluated through direct recruitment of effectors, rather than implying a comparison between disparate signaling outputs.

> *(3) Abstract, line 34: The term "balanced agonist" should be removed. Any chosen reference ligand is, by definition, the "balanced" agonist for that analysis, regardless of its actual signaling profile. Consequently, the expression "balanced agonist" adds no mechanistic information beyond "the agonist used as reference in a particular bias*

> *calculation" and is potentially misleading, as it implies that this ligand possesses a uniquely unbiased, system-independent signaling profile, which is not the case.*

We agree with the reviewer that the term “bias” is always relative to a specific reference ligand. Indeed, it is known that some natural chemokine:receptor pairs show some bias on its own. Therefore, we adjusted the text in the abstract on Pg.2 and removed the word “balanced”.

> *(4) Abstract, line 36: I also recommend removing the term "bias" at this point. The concept of bias typically arises from experiments that quantitatively compare more than one variable. As currently written, the phrasing suggests a dichotomy between G protein- and arrestin-mediated signaling, yet the study does not assess arrestin signaling, only arrestin recruitment. Under these conditions, the use of "bias" is not appropriate. The data are clear and compelling on their own without the need for this potentially misleading terminology.*

We thank the reviewer for this comment. We would like to emphasize that our conclusions are based on the fact that we measure both G protein (mGi recruitment) and arrestin (arrestin recruitment) as protein:protein interactions. We have changed the text in the abstract on pg.2 to further distinguish between signaling and recruitment:

“Additionally, G protein recruitment to CCR9 was unimpeded by VUP25111, suggesting that the miniprotein biased the native agonist towards G proteins.”

> *(5) Introduction: This is interesting to read and generally well written, though certain statements would benefit from improved semantic precision. For example, in lines 110-111, the phrase "G protein-biased complex" should be reconsidered, as it relies on the notion of G protein- versus arrestin-mediated signaling. Arrestins themselves do not signal; what is measured here is their recruitment. Comparing G protein signaling with arrestin recruitment is therefore conceptually unsound, since arrestin engagement is a downstream consequence of G protein activation. Comparisons become meaningful only when designed to differentiate between G protein-dependent and G protein-independent arrestin recruitment, which is not the case in this study.*

Since the VUP25111:CCL25 complex suppresses arrestin recruitment to CCR9, but not G protein recruitment, we are confident representing the modified agonist as G protein-biased. Additionally, arrestin recruitment is only downstream of G protein activation in the occasion where the GPCR is phosphorylated specifically by GRK2/3 and not GRK5/6. CCR9 does not show any preference for GRKs and recruits arrestin as effectively when phosphorylated by either GRK2/3 or GRK5/6 (Lamme JBC 2025). Since G protein coupling is preserved when challenged with the VUP25111:CCL25 complex, both families of GRKs should be available for phosphorylation. We have modified the statement to better specify recruitment compared to signaling on Pg. 5:

“Most prevent activation by impeding chemokine binding to the receptor, thus impairing all signaling and migratory responses, but one forms a G protein-biased complex with CCL25, preserving G protein recruitment while suppressing arrestin recruitment to CCR9, and selectively inhibits CCR9, but not ACKR4.

> *(6) Results, 122,123: The authors should consider being more precise; possibly, the truncated CCL25 is somewhat less potent on CCR9. The authors should make a statistical test and then decide whether to rephrase or not for enhanced precision.*

The reviewer is correct that we detect a small difference in potency between full-length CCL25 and CCL25-ΔCT at CCR9. This was quantified and is reported in the supplementary Table S2, where CCL25 shows a logEC50 of -7.46 ± 0.16 compared with -7.89 ± 0.29 for CCL25-ΔCT, indicating that the truncated chemokine is slightly more potent. While the difference

was determined to be statistically significant per an Extra sum-of-squares F test, we don't consider the of the truncation to be substantially impactful, which is also in line with previous publication (Pinheiro Nat. Comm. 2025). We have therefore revised the text to note the modest increase in potency of CCL25-ΔCT compared to the native, full-length CCL25 and added statistical information in the figure legend. We have changed the text on Pg. 5 to:

"The truncated CCL25 (CCL25_ΔCT, 1-77) activated both CCR9 and ACKR4 with similar efficacy while showing slightly enhanced potency only towards CCR9 compared to the full-length ligand (Fig. S1)."

> *(7) Figure S5: This figure is currently confusing and needs clarification. The authors state in the main text that CXCR4 is stimulated with CXCL12, yet the figure legend refers to CCL25; this discrepancy should be corrected to ensure consistency. In addition, inhibition of CXCR4 by the miniprotein binders should be analyzed and presented with normalization to CXCR4 responses, not to CCL25-stimulated CCR9. To avoid misinterpretation, inhibition by the miniproteins should be quantified separately for CCR9 and CXCR4, each normalized to its own receptor-specific and functionally equivalent stimulation condition, rather than to the "other" receptor.*

We thank the reviewer for this comment and apologize for the oversight during editing. The mentions of CCL25 in Figure S5 were incorrect, and CXCL12 was indeed used in this cross-reactivity assay to stimulate CXCR4 and for subsequent normalization. We have adjusted the legend accordingly.

> *(8) Results, lines 211-213: The authors should be more semantically precise. They state that no binder has any effect on arrestin recruitment to CXCR4. If I see the data, this is not really true, as 25101 and 25107 inhibit arrestin recruitment by about 50 % or more at the highest applied concentrations; only 111 and 112 are completely inactive. As already commented, normalization should be done to arrestin recruitment of CXCR4 and not CCR9.*

We thank the reviewer for this comment and agree that, at the highest tested concentrations of VUP25101 and VUP25107, substantial inhibition is observed. Additionally, we have extended our analysis of the miniprotein selectivity to include activation assays for the CCL20 receptors CCR6 and ACKR4, as well as the atypical CXCL12 receptor ACKR3. Based on these data, we have revised the text to more accurately reflect these observations. We now frame these results as an initial proof of concept demonstrating the feasibility of this design approach, while noting that further optimization and characterization of selectivity will be required to advance the miniproteins for additional applications.

We have adjusted the text on Pg.11:

"CCL25 specificity was experimentally evaluated by testing the miniproteins against CXCL12 by tracking arrestin recruitment to CXCR4 and ACKR3, the native agonist for this canonical and atypical receptor pair (Fig. S5). VUP25111 and VUP25112 showed no effect on CXCL12-mediated activation at any concentration, while VUP25101 and VUP25107 showed partial inhibition at the highest tested concentration (10 μM).

In addition, the effects of the VUPs were evaluated against CCL20, a closely related chemokine to CCL25, by assessing arrestin recruitment to CCR6 and ACKR4 (Fig. S6). VUP25107 and VUP25112 displayed similar potencies towards CCL20 comparable to those observed for CCL25 (VUP25107: pIC50 = 7.72 ± 0.21; VUP25112: pIC50 = 6.93 ± 1.03) to ACKR4. In contrast, VUP25101 showed reduced inhibition of CCL20 relative to CCL25 (VUP25101: $pIC50_{CCL20}$ = 6.06 ± 0.13 v $pIC50_{CCL25}$ = 7.73 ± 0.08), indicating greater selectivity. CCL20 activation of CCR6 further supports the specificity of VUP25101, which only showed a modest effect at the highest concentration tested. VUP25111 showed no inhibitory effects on CCL20 activation of

either CCR6 nor ACKR4, which may indicate a lack of binding, but is indiscernible from forming a receptor-competent complex similar to how it interacts with CCL25 and ACKR4."

Concerning the comment regarding the normalization to CCR9 rather than CXCR4, due to a mistake, the figure legend incorrectly stated CCL25, whereas the assay was performed using CXCL12. We thank the reviewer for bringing this up and have corrected the figure accordingly.

https://doi.org/10.7554/eLife.111190.2.sa0